A

PROJECT WORK

ON

A REVIEW ON COPPER NANO CLUSTERS DOPED WITH TRANSITION METALS AND ADSORBED WITH TOXIC GASES BY COMPUTATIONAL METHODS

SUBMITTED FOR THE PARTIAL FULFILLMENT OF THE REQUIREMENT FOR

THE AWARD OF THE DEGREE OF

M.Sc. (Physics)

SUBMITTED BY

SHAIK ARSHAD

Roll No. 108923509012

G. PULLA REDDY DEGREE & PG COLLEGE

(Affiliated to Osmania University)

An Iso 9001:2015 Certified Institution

Mehdipatnam, Hyderabad-28

Academic Year (2024-2025)

G. PULLA REDDY DEGREE & P.G COLLEGE

(Affiliated to Osmania University)

An Iso 9001:2015 Certified Institution

Mehdipatnam, Hyderabad-28

Academic Year (2024-2025)

CERTIFICATE

This is to Certified that Bonafide practical work on **"A review on copper nano clusters doped with transition metals and adsorbed with toxic gases by computational methods"** is done by SHAIK ARSHAD Bearing Roll No. 108923509012 Studying in M.Sc. (Physics), IV Semester for the Academic Year 2024-2025.

This Project work is submitted as the partial fulfilment of the requirement of the degree of M.Sc. (Physics) for the Academic year **2024-2025**.

Project Guide **External Examiner**

DECLARATION

I hereby declare that the work presented in this Project Report has been carried out by me along with my project guide KUMBAGIRI MADHAVI. As a partial fulfilment for the award of the degree of M.Sc. (Physics) and submitted to the DEPARTMENT OF PHYSICS and further declare that neither this Project nor any part of this Project Report has been submitted for any Degree/Diploma or any other award anywhere before.

Signature of the Student :

Name of the Student : SHAIK ARSHAD

Hall ticket number : 108923509012

ACKNOWLEDGEMENTS

I take this opportunity to express my deep sense of gratitude and heartful thanks to several key personalities whose constant support and encouragement have helped me to transfer my effort into the completion of this project.

I am grateful to the Principal, **Dr. K. Murali Krishna** and the Department of Physics at the GPRDPGC for giving me the opportunity to execute this project, which is an integral part of the curriculum.

I express my deepest gratitude to my project guide Mrs. **KUMBAGIRI MADHAVI** whose guidance, encouragement, and support from the initial to the final level enabled me to develop and understanding of the subject.

Finally, I would like to express my deepest appreciation to my parents, family members and friends and the most precious people in my life for their confidence in me and for the support, love and understanding that they have provided me throughout my life.

CONTENTS

LIST OF TABLES

LIST OF FIGURES

A REVIEW ON SENSING OF COPPER NANO CLUSTERS DOPED WITH TRANSITION METALS AND ADSORBED WITH TOXIC GASES BY COMPUTATIONAL METHODS

Abstract

The present study investigates the interactions of environmental pollutants, such as CO, NO, and, with copper nanoclusters Cu_n (n=2-6), given their significant applications in catalysis and gas sensing. Among the nanoclusters studied, Cu_4 and Cu_6 demonstrated the strongest interactions with toxic gases and exhibited aromatic properties. When alloyed with silver (Ag) and nickel (Ni) to form bimetallic nanoclusters (Cu_3M and Cu_6M, where M = Ag, Ni), these clusters displayed enhanced catalytic activities for gas sensing, storage, and removal of harmful chemicals. The study calculated the structural stability, infrared activity, formation energy, and binding energies of Cu_4 and Cu_6 clusters alloyed with Ag and Ni, yielding values of -2.82 eV, -3.26 eV, -3.32 eV, and 3.62 eV, respectively. These results indicate that interactions with transition metals (TMs) are energetically favourable. The calculated adsorption energies for CO gas on pristine Cu_4, Cu_3Ag, and Cu_3Ni were determined to be -0.60, -0.40, and -0.56 eV, respectively, indicating weak physisorption in the case of Cu_3Ag. Similarly, the adsorption energies for NO gas on Cu_4, Cu_6, and Cu_3Ag were -0.79, -0.21, and -0.77 eV, respectively. Furthermore, NH_3 adsorption on Cu_3Ag resulted in an energy of -1.11 eV, suggesting stronger interaction compared to other gases. The optimal adsorption energy obtained suggests promising recovery times for CO and NO on Cu_3Ni and Cu_6, measured at 2.20 and 2.70 seconds, respectively, underscoring their effectiveness in molecular sensing. For NH_3, the recovery time of 3.85 seconds highlights the potential of both doped and pristine clusters for efficient NH_3 removal from the environment. Additionally, the study analysed the density of states (DOS), revealing significant changes in molecular orbitals, particularly in the HOMO-LUMO gap, which further supports the enhanced reactivity of the nanoclusters.

Keywords: Hazardous gas, Alloyed Cu cluster, Gas sensing, Density Functional theory

CHAPTER I

Introduction

1.1 Introduction

Nanoscale Science and Engineering proffers opportunities to address variety of ongoing scientific and technological challenges. Nanotechnology has played a pivotal role in advancing several fields like healthcare industry, material science research, improved solar energy, environmental science and driving innovations and unlocking many other applications [1-6]. Nanomaterials, with sizes ranging from 1 to 100 nm, exhibit special effects like the quantum size effect, high surface-to-volume ratio, tunable optical properties, enhanced catalytic activity, macroscopic quantum tunnelling effect and high bioactivity at low temperature. Over the years, Metal nanoclusters (NCs) have garnered significant research interest in recent years due to their distinct optical and physical properties.

Typically, these nanoclusters possess a diameter of approximately 2 nanometre and consist of metallic cores with between 10 and 100 metal atoms, the quantum confinement effect in metal nanoclusters leads to the discretization of electronic energy levels, which is a departure from the continuous bands seen in bulk materials. This effect arises due to the reduced size of the NCs, which confines the electrons to a smaller space, leading to the quantization of their energy states. As a result, metal NCs exhibit distinctive electronic transitions that are more akin to those observed in molecules. These transitions are characterized by discrete energy levels, which give rise to the unique optical and electronic properties of metal NCs. The size-dependent nature of these properties means that by controlling the size of the NCs, one can tune their electronic transitions and, consequently, their optical responses such as fluorescence emission. This phenomenon underpins the use of metal NCs in various applications, including catalysis, imaging, and sensing [7] where their distinct electronic transitions play a crucial role that make them extremely versatile and valuable in a wide range of fields, including medicine, electronics, energy, and environmental science, sensing technologies.

Amongst the transition metal based NCs viz, platinum (Pt), gold (Au), and silver (Ag), those based on copper (Cu) have attracted peculiar interest on account of the high earth abundance, low cost, and low toxicity of Cu.[8] Copper metal nanoclusters(CuNCs), in particular, stand out for their unique chemical and physical properties, which make them highly useful in a variety of applications, including therapeutics, medical diagnostics, nanodevices, chemical sensors, catalysis, and more [9].

Copper belonging to d-Block elements possess high electrical conductivity, malleability and appear shiny [10] with variable valence state, it becomes a highly significant catalyst and holds immense promise for extensive application in the fields of both thermal catalysis and electrocatalysis [11-23]. Without the Question, the interplay between the composition and

structure of CuNCs underpins their multifaceted roles and potential in diverse technological and scientific applications. Single phase metals like copper have increased tendency of oxidation to generate metallic oxide compounds which in turn act like a self-protective layer over metals. Due to this the electroconductive nature of copper decreases thereby specifying the issues metal alloys such as silver (Ag), gold (Au) and platinum (Pt) are used to form bimetallic nanoparticles with copper [24-26]. This transition metal nanocluster has motivated the interest in researchers for detecting the behavior of alloys and possibilities to alter the nanoclusters. To enhance the catalytic activities, alloying play a vital role in modifying the properties of nanoclusters [27,28] or regulating the magnetic properties [29,30].

Many researches indicate on beneficial effect of using transition metal alloys [31]. The geometrical changes on the upper most surface of the nanocluster leads to the development of multiple facets, edges, corners and defects which creates an additional reactive site. Due to intense binding energy of the core electrons are significant and are greatly influenced by the interactions between surface sites and reactants. The deposition of secondary metals provides a peculiar catalytic activity which are not available in monometallic particles. So, by deposition of secondary metals the modification in the electrical properties as well as chemical reactivity of a surface is improved [32]. The catalytic activity with bare Pt /Ni and Pd/Ni clusters showed a notable intensification when Fe/ Ru alloys have improvement over pure iron catalyst (Fischer - Tropsch synthesis). In a very recent experimental study, [33] it was observed that carbon supported small Cu_n (n = 3, 4) clusters are more efficient for electrocatalytic reduction of CO_2 to ethanol. Moreover, the use of a Cu_4 cluster supported on various surfaces is not limited to methanol or ethanol synthesis only; Cu_4 can also serve as an efficient catalyst for the conversion of CO_2 to products like carbon monoxide and methane, as well as in acetylene trimerization when supported on SiO_2. Yun, W. S. & Lee, J. D. depicted tetrahedral structure of four Cu atoms (Cu_4) shows more stability due to the strong chemical bonds among Cu_4 when inserted into MoS_2.

Similarly, bonding is observed in Cu_6 with dopants like Sc [34]. Increasing investigations into metallic and bimetallic nanoclusters have been driven by their promising catalytic activity, potential use in biosensors, and unique electronic properties. Nguyen and co-workers [35-36] and Matulis et al. have studied the electronic structure, stability, and geometry of cationic and anionic pure and bimetallic copper clusters. Their research likely focused on understanding how the electronic configurations and interactions within these clusters influence their stability and geometric arrangements, which are critical for their potential applications in catalysis, electronics, and other fields.

For the adsorption of toxic gases; several nanoclusters have been designed based on metals like gold (Au) [37-38] palladium (Pd) [39], rhodium (Rh) [40], vanadium(V) [41] and platinum (Pt) [42]. Environmental concerns, such as the emission of toxic gases like carbon monoxide (CO), nitrogen oxides (NO_x), and ammonia (NH_3) from industrial activities, have driven the development of advanced gas sensors. These sensors, leveraging the unique properties of CuNCs, exhibit high sensitivity, selectivity, and the capability to detect gases at low concentrations, thus contributing to environmental protection and public health. Illas et al. [43-44] reported the theoretical results of bonding mechanism of NO to Cu(1 1 1) cluster, while Balkenende et al. [45] and Dumas et al. [46] presented the experimental data of NO reactions on Cu(1 1 1). Recently, González et al. [47] showed theoretically that NO desorption could occur prior to the N–O dissociation. The work points towards the possibility of controlling adsorption sites through tailored surface compositions, offering a promising avenue for tuning catalyst performance in bimetallic systems

The present work will focus on the use of CuNCs in its pristine form and alloying with Ag, Ni nanoparticles (NPs) to fabricate bimetallic nanocluster for increased sensing and improved stability. Our study will shed new light on the rational design of high-performance nanomaterials gas sensors by harnessing the synergetic effects of different materials.

In this work, we investigated the adsorption of toxic gases on pure and bimetallic copper clusters using a first principles approach. Specifically, the gases studied include CO, NO, NH_3, which have not been extensively studied in existing literature onto copper cluster and alloyed copper clusters. The study of adsorption energies, DOS, electronic properties, charge transfer, work function and recovery time recommended that the copper nanoclusters could have potential applications as toxic gas sensor. The present work is arranged in the following manner. In Section 2, we describe the computational methods employed for performing the calculations to study the properties of pristine Cu Cluster and Bimetallic cluster–molecule complexes. This section also provides information about the methods employed via state of art Density Functional theory in a Gaussian Software. Section 3 is devoted to the discussion on the results obtained by employing the DFT-based methods. In Section 4, we conclude the present work.

CHAPTER II

Computational Details

Gaussian 09 package to optimize and calculate pristine and Ag, Ni doped Cu_4 and Cu_6 nanoclusters [48] is used. All the calculations were performed using DFT/B3LYP with Grimme's-D3 [49] method to include dispersion correction term. Furthermore, we used LanL2DZ basis sets. The infrared frequency has also been calculated and plotted to see the stability of the structure, where we considered global charge as zero, indicating neutrality.

The computation of Natural Bond Orbital (NBO) is also carried out in order to facilitate the analysis of charge transfer direction and the retrieval of different maps of electronic densities along with Mulliken charge analysis. In addition, calculation of the HOMO-LUMO gap or more precisely band gap is also achieved by calculating the difference between the highest occupied molecular orbital and the lowest unoccupied molecular orbital and the equation is

$$E_g = E_{LUMO} - E_{HOMO} \quad \text{..... (1)}$$

The fermi energy is calculated by

$$E_F = \frac{E_{HOMO}+E_{LUMO}}{2} \quad \text{..... (2)}$$

Where E_{LUMO} & E_{HOMO} are energies of LUMO and HOMO energy levels. Utilizing Gauss View 5.0 software, visualization of the structure, highest occupied molecular orbital (HOMO), lowest unoccupied molecular orbital (LUMO), Mulliken charge distribution, and Molecular Electrostatic Potential (MEP) surface of the molecules has been done. To obtain density of states (DOS) and IR spectra, Gauss Sum software was utilized.

2.1 Density Functional Theory (DFT)

Density Functional Theory (DFT) is a computational quantum mechanical modelling method used to investigate the electronic structure of many-body systems, particularly atoms and molecules. It has become a cornerstone in modern physics and chemistry, enabling researchers to study complex systems with unprecedented accuracy. The fundamental idea behind DFT is to describe the ground state of a system using the electron density, rather than the many-body wave function. This approach was pioneered by Hohenberg and Kohn (1964) and later developed by Kohn and Sham (1965). The Hohenberg-Kohn theorem states that the ground-state density of a system determines its ground-state properties, including the energy. [1-2]

1. The Hohenberg-Kohn Theorem: Establishes the relationship between the ground-state density and the ground-state energy.

2. The Kohn-Sham Equations: A set of single-particle equations that allow for the calculation of the ground-state density and energy.
3. Exchange-Correlation Functional: A crucial component of DFT that accounts for the exchange and correlation effects between electrons.

2.1.1 Applications of DFT

1. Materials Science: DFT has been used to study the properties of metals, semiconductors, and insulators, including their electronic structure, lattice constants, and phase transitions.
2. Chemistry: DFT has been employed to investigate the properties of molecules, including their geometries, vibrational frequencies, and reaction energies.
3. Biological Systems: DFT has been used to study the properties of biomolecules, such as proteins and DNA, and their interactions with other molecules.[1]

2.1.2 Advantages and Limitations of DFT

Advantages:

- Computational Efficiency: DFT is generally more computationally efficient than other quantum mechanical methods, such as post-Hartree-Fock methods.
- Accuracy: DFT can provide accurate results for a wide range of systems, including metals and semiconductors.[2]

Limitations

- Approximations: DFT relies on approximations, such as the local density approximation (LDA) and the generalized gradient approximation (GGA), which can lead to errors in certain systems.
- Strongly Correlated Systems: DFT can struggle to describe systems with strong electronic correlations, such as transition metal oxides.[1]

2.2 BASIS SET

In quantum chemistry and computational physics, a basis set refers to a set of functions used to describe the electronic wavefunctions of a system, typically within the framework of the Hartree-Fock or Density Functional Theory (DFT) methods. These functions are combined to approximate the wavefunctions of electrons in atoms, molecules, or solids.

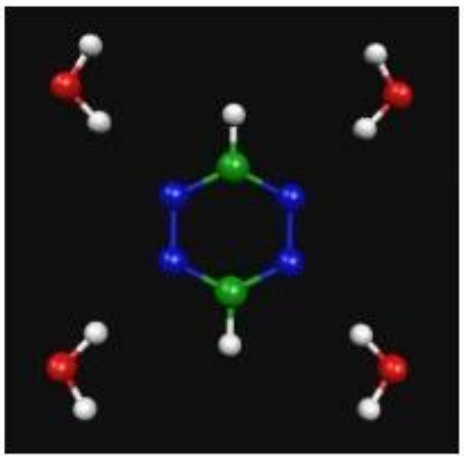

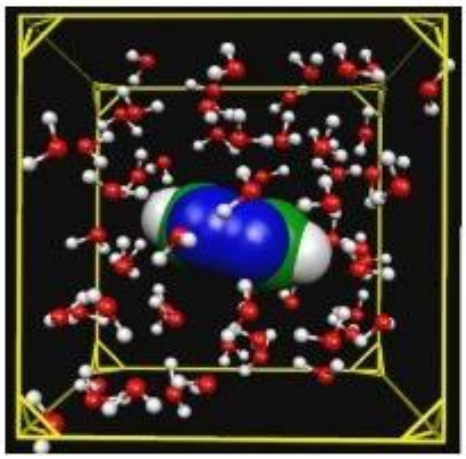

2.2.1 Types of Basis Functions:

Gaussian-type Orbitals (GTOs): These are the most common basis functions in quantum chemistry. They are computationally efficient due to their simple mathematical properties but may require a larger number of functions to achieve high accuracy.

Slater-type Orbitals (STOs): These more closely resemble the true shape of atomic orbitals but are computationally more demanding.

2.2.2 Basis Set Families:

Minimal Basis Sets: These use the smallest number of functions necessary to describe each electron in the system (e.g., STO-3G).

Split-Valence Basis Sets: These offer more flexibility by using multiple functions for valence electrons, which are more chemically active (e.g., 6-31G).

Polarized Basis Sets: These include additional functions (like d- or f-type orbitals) to better describe electron distribution in non-spherical environments (e.g., 6-31G*).

Diffuse Basis Sets: These contain functions with smaller exponents to describe electron density far from the nucleus, useful for anions or molecules with loosely bound electrons (e.g., 6-31+G*).

Usage:

The choice of a basis set affects the accuracy and computational cost of quantum chemical calculations. Larger and more flexible basis sets generally provide more accurate results but at a higher computational expense.

2.3LANL2DZ Basis Set

The LANL2DZ basis set is a popular choice for DFT calculations, particularly for systems involving transition metals and heavier elements.

The acronym LANL2DZ stands for Los Alamos National Laboratory 2 Double Zeta.

2.3.1 Effective Core Potential (ECP):

Core Electrons: For elements with a high atomic number (typically beyond the first-row transition metals), the LANL2DZ basis set uses an Effective Core Potential (ECP): This replaces the core electrons with a potential that mimics their effect, simplifying calculations by reducing the number of electrons explicitly considered in the quantum mechanical treatment.

Valence Electrons: Only the valence electrons are treated explicitly with a Gaussian-type basis set, while the ECP accounts for the core electrons.

Double-Zeta Basis Set:

The "2DZ" part of the name indicates that the valence orbitals are described using a double-zeta basis set, meaning there are two sets of functions for each valence orbital. This allows for a more flexible and accurate description of the valence electron distribution compared to a minimal or single-zeta basis set.

The LANL2DZ basis set is a double-zeta basis set that includes effective core potentials (ECPs) for transition metals. It was developed by Los Alamos National Laboratory (LANL) and is widely used in DFT calculations.[4]

2.3.2 Advantages of LANL2DZ Basis Set

1. Accuracy: The LANL2DZ basis set provides a good balance between accuracy and computational efficiency.
2. Transition Metals: The LANL2DZ basis set is particularly useful for systems involving transition metals, as it includes ECPs that account for relativistic effects.
3. Computational Efficiency: The LANL2DZ basis set is computationally efficient, making it suitable for large systems.

2.3.3 Applications

1. Transition Metal Complexes: The LANL2DZ basis set is widely used to study the properties of transition metal complexes, including their geometries, vibrational frequencies, and electronic structures.
2. Catalysis: The LANL2DZ basis set is used to investigate the mechanisms of catalytic reactions involving transition metals.
3. Materials Science: The LANL2DZ basis set is applied to study the properties of materials, including their electronic structures, lattice constants, and phase transitions.

2.3.4 DFT Calculations with LANL2DZ Basis Set

1. Geometry Optimization: DFT calculations with the LANL2DZ basis set can be used to optimize the geometries of molecules and solids.
2. Vibrational Frequencies: DFT calculations with the LANL2DZ basis set can be used to calculate vibrational frequencies, which are important for understanding the thermodynamic properties of systems.
3. Electronic Structure: DFT calculations with the LANL2DZ basis set can be used to investigate the electronic structure of systems, including their molecular orbitals and density of states.

2.3.5 GAUSSIAN SOFTWARE

Gaussian window specifying the tools required for performing the geometric calculations of the electronic structure. Here in the file menu bar selecting the new molecule with the help of builder we can design the necessary molecule as shown in builder tab.

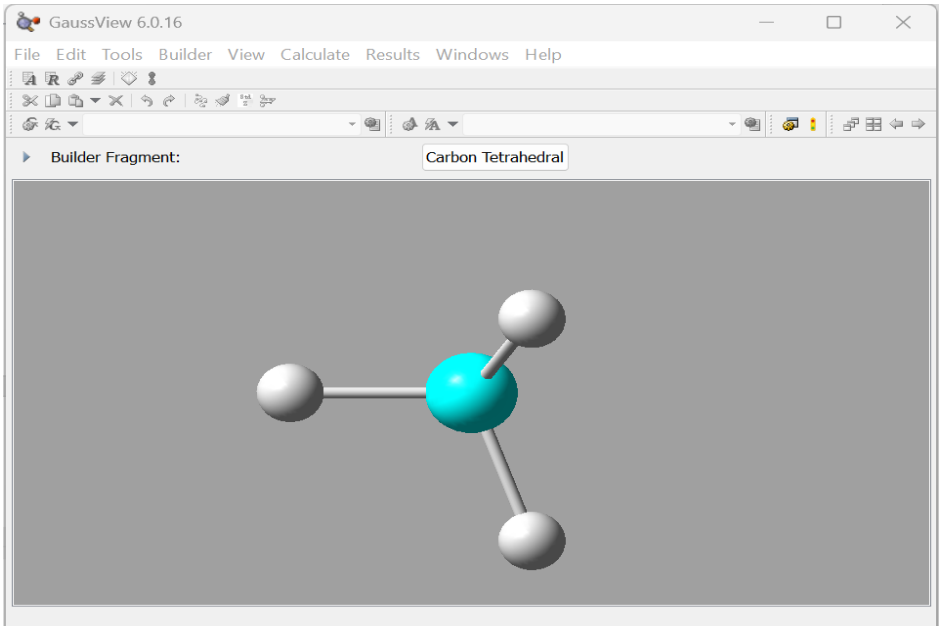

FIG 1.1 Gauss View

Gaussian is a computational chemistry software package widely used for molecular modelling and quantum chemical calculations. The Builder module is a key component of Gaussian, enabling users to create and manipulate molecular structures.

Features of Builder

1. Molecular Structure Creation: The Builder allows users to create molecular structures from scratch or import existing structures from various file formats.

2. Molecular Editing: Users can edit molecular structures, including adding or removing atoms, modifying bond lengths and angles, and adjusting dihedral angles.

3. Visualization: The Builder provides a graphical interface for visualizing molecular structures, enabling users to inspect and analyze their systems.

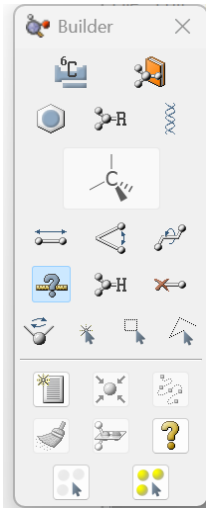

FIG 1.2 Builder

Gaussian is a computational chemistry software package that offers a range of tools for molecular modeling and quantum chemical calculations. Element fragments are a useful feature in Gaussian, enabling users to build molecular structures efficiently.

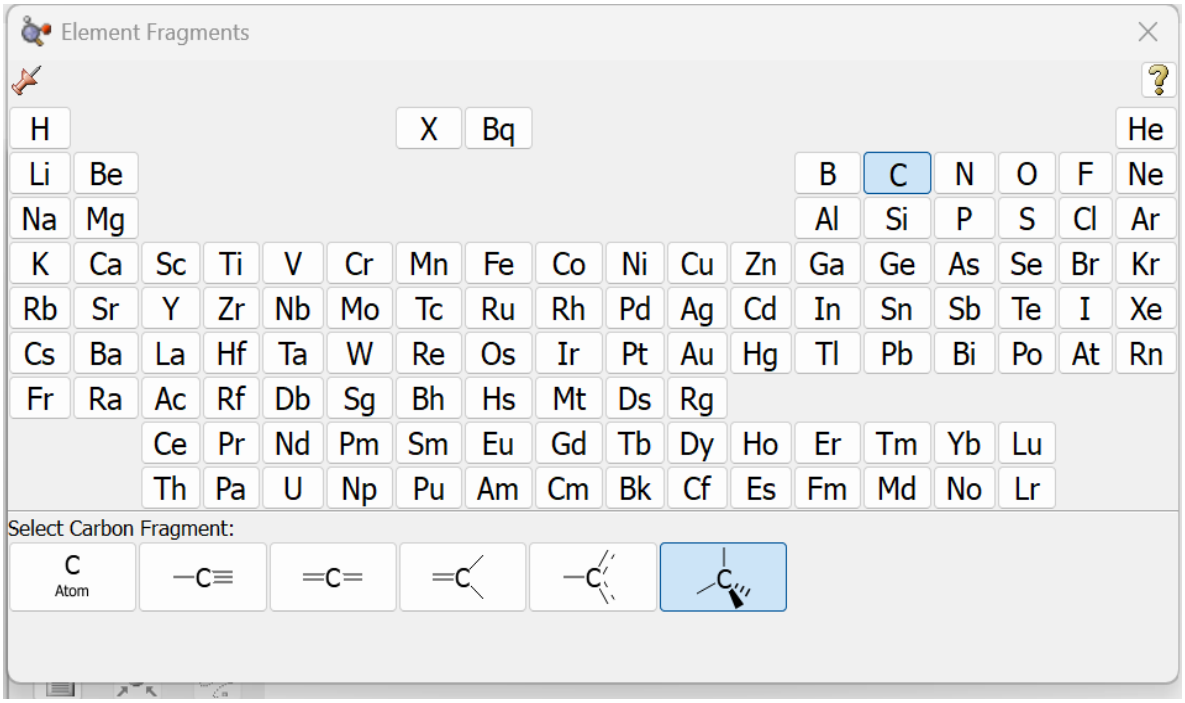

FIG 1.3 Element Fragments

Features of Element Fragments

1. Pre-defined Fragments: Gaussian provides pre-defined element fragments, such as functional groups and molecular building blocks.

2. Customizable: Users can create and save their own custom element fragments for future use.

3. Easy Integration: Element fragments can be easily integrated into molecular structures, streamlining the building process.

2.3.6 OPTIMISED STRUCTURE

In Gaussian software, an optimized structure refers to a molecular geometry that has been optimized to minimize its energy. This is achieved through quantum chemical calculations, which adjust the positions of atoms to find the most stable arrangement.

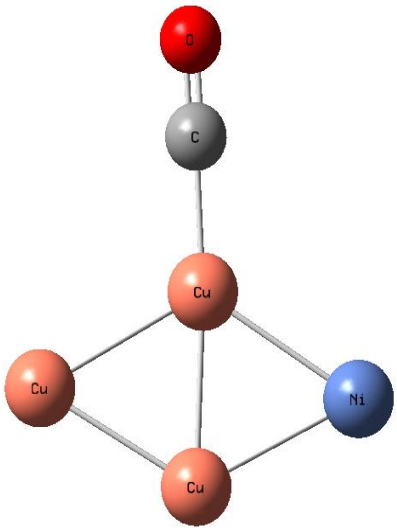

FIG 1.4 Optimize Molecule

Optimization Process

1. Initial Guess: The user provides an initial guess of the molecular structure.

2. Energy Calculation: Gaussian calculates the energy of the molecule using quantum chemical methods (e.g., Hartree-Fock, DFT).

3. Geometry Optimization: The software iteratively adjusts the molecular geometry to minimize the energy, using algorithms such as Berny optimization or steepest descent.

In Gaussian software, bond structure refers to the arrangement of atoms and bonds within a molecule. Gaussian allows users to define and manipulate bond structures, including bond lengths, angles, and dihedral angles.

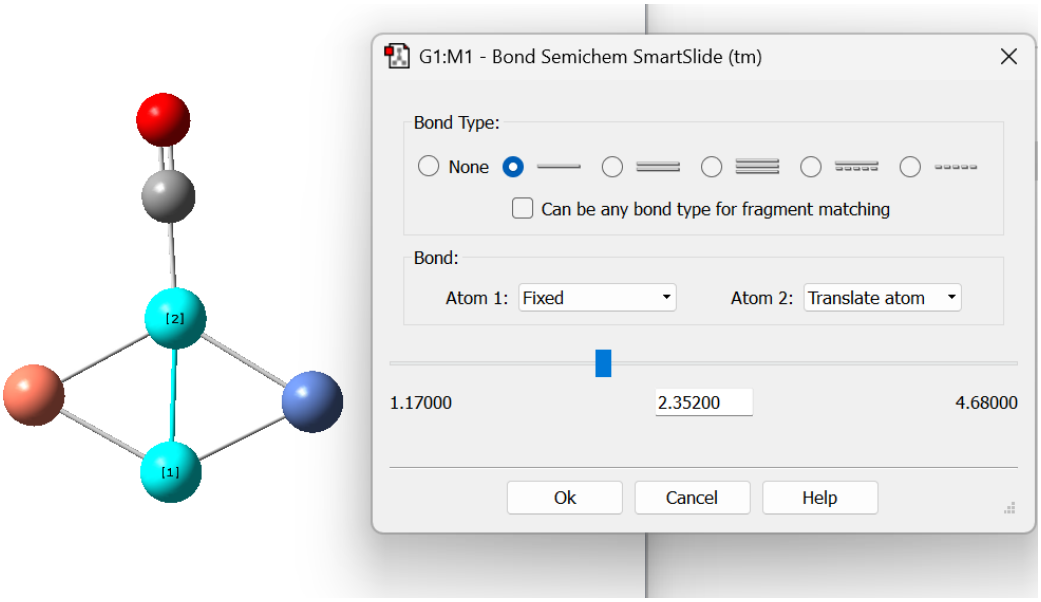

FIG 1.5 Bond Builder

Key Features

1. Bond Lengths: Gaussian allows users to specify bond lengths, which can be optimized during geometry optimization calculations.

2. Bond Angles: Users can define bond angles, which are critical in determining molecular shape and properties.

3. Dihedral Angles: Gaussian enables users to specify dihedral angles, which describe the rotation of atoms around bonds.

FIG 1.6 .chk File Summary

Title Card Required		
C:/Users/KUMBAGIRI MADHAVI/Downloa...		
File Type	.chk	
Calculation Type	FREQ	
Calculation Method	UB3LYP	
Basis Set	LANL2DZ	
Charge	0	
Spin	Doublet	
Solvation	scrf=check	
Electronic Energy	-871.122381	Hartree
RMS Gradient Norm	0.000021	Hartree/Bohr
Imaginary Freq		
Dipole Moment	0.830852	Debye
Polarizability (α)	172.431737	a.u.
Point Group		

FIG 1.7 .log File Summary

Title Card Required		
C:/Users/KUMBAGIRI MADHAVI/Downloa...		
File Type	.log	
Calculation Type	FREQ	
Calculation Method	UB3LYP	
Basis Set	LANL2DZ	
Charge	0	
Spin	Doublet	
Solvation	None	
E(UB3LYP)	-871.122381	Hartree
RMS Gradient Norm	0.000021	Hartree/Bohr
Imaginary Freq	0	
Dipole Moment	0.830870	Debye
Polarizability (α)	172.431667	a.u.
Point Group	CS	
Job cpu time:	0 days 0 hours 2 minutes ...	

Gaussian software generates two important files during calculations: the checkpoint file (.chk) and the log file (.log). These files provide valuable information about the calculation.

CHK File Summary

1. Binary data: Stores molecular geometry, basis set, and wavefunction information.
2. Restart calculations: Allows users to restart calculations from a previous point.

Log File Summary

The log file (.log) contains:

1. Calculation details: Records calculation settings, molecular geometry, and convergence information.
2. Energy values: Reports energy values, including total energy, kinetic energy, and potential energy.
3. Optimization progress: Tracks optimization progress, including geometry convergence.

HOMO (Highest Occupied Molecular Orbital) and LUMO (Lowest Unoccupied Molecular Orbital) are crucial in understanding molecular electronic structure. The HOMO-LUMO gap is a key descriptor of molecular reactivity and stability.

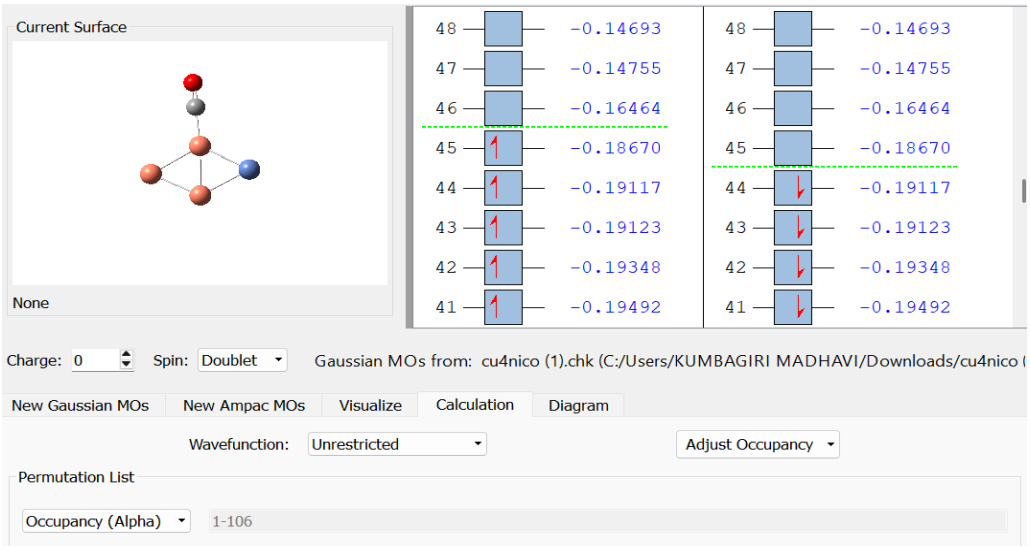

FIG 1.8 Alpha Beta Orbitals in unrestricted wave function

Alpha and Beta Orbitals

In Gaussian software, alpha and beta refer to the spin orbitals in an unrestricted calculation:

1. Alpha Orbitals: Alpha orbitals correspond to electrons with spin up (↑).
2. Beta Orbitals: Beta orbitals correspond to electrons with spin down (↓).

2.4 HOMO (HIGHEST OCCUPIED MOLECULAR ORBITALS)

In Density Functional Theory (DFT), the Highest Occupied Molecular Orbital (HOMO) is the molecular orbital with the highest energy that is occupied by electrons in the ground state of a molecule or system.

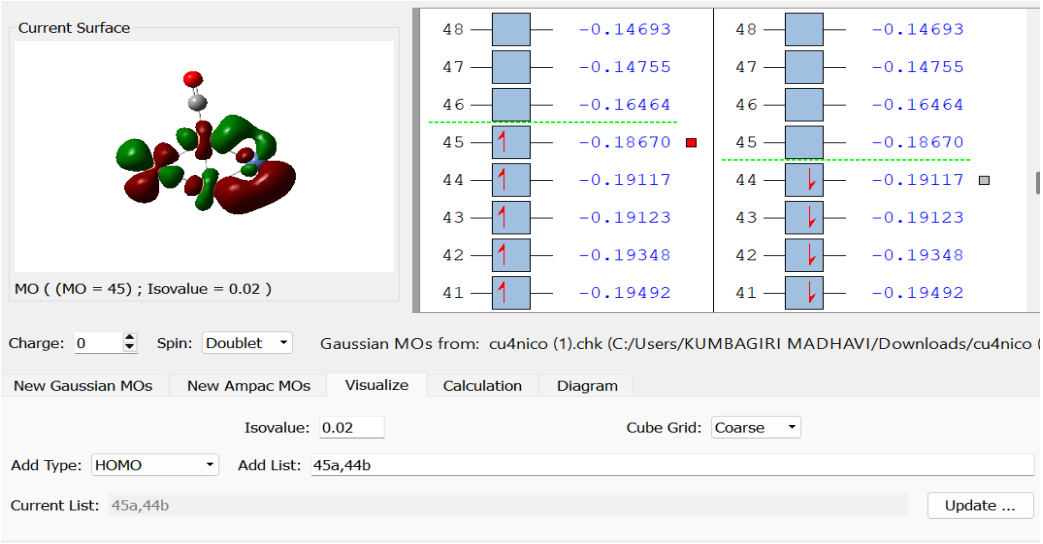

FIG 1.9 HOMO Orbital

Definition:

HOMO: Represents the topmost orbital that contains electrons. It is crucial for understanding a molecule's electronic structure and reactivity.

Units:

Energy levels of HOMO are typically given in electron volts (eV) or atomic units (a.u.), depending on the context and computational method.

2.4.1 DFT Calculation:

Determine HOMO Energy: After solving the Kohn-Sham equations, the energy of the HOMO can be found from the energy levels of the occupied Kohn-Sham orbitals.

Procedure: Perform a self-consistent DFT calculation to obtain the Kohn-Sham orbitals, then identify the highest energy orbital among those occupied.

Applications:

Chemical Reactivity: The HOMO energy is used in the frontier molecular orbital theory to predict reactivity and interaction sites in chemical reactions.

Spectroscopy: HOMO levels can influence UV-Vis absorption spectra and other electronic transitions.

Material Design: Important in designing materials for organic electronics and photovoltaics, where the energy of the HOMO affects charge injection and transport.

2.5 LUMO (LOWEST UNOCCUPIED MOLECULAR ORBITAL)

In Density Functional Theory (DFT), the Lowest Unoccupied Molecular Orbital (LUMO) is the molecular orbital with the lowest energy that is not occupied by electrons in the ground state of a molecule or system.

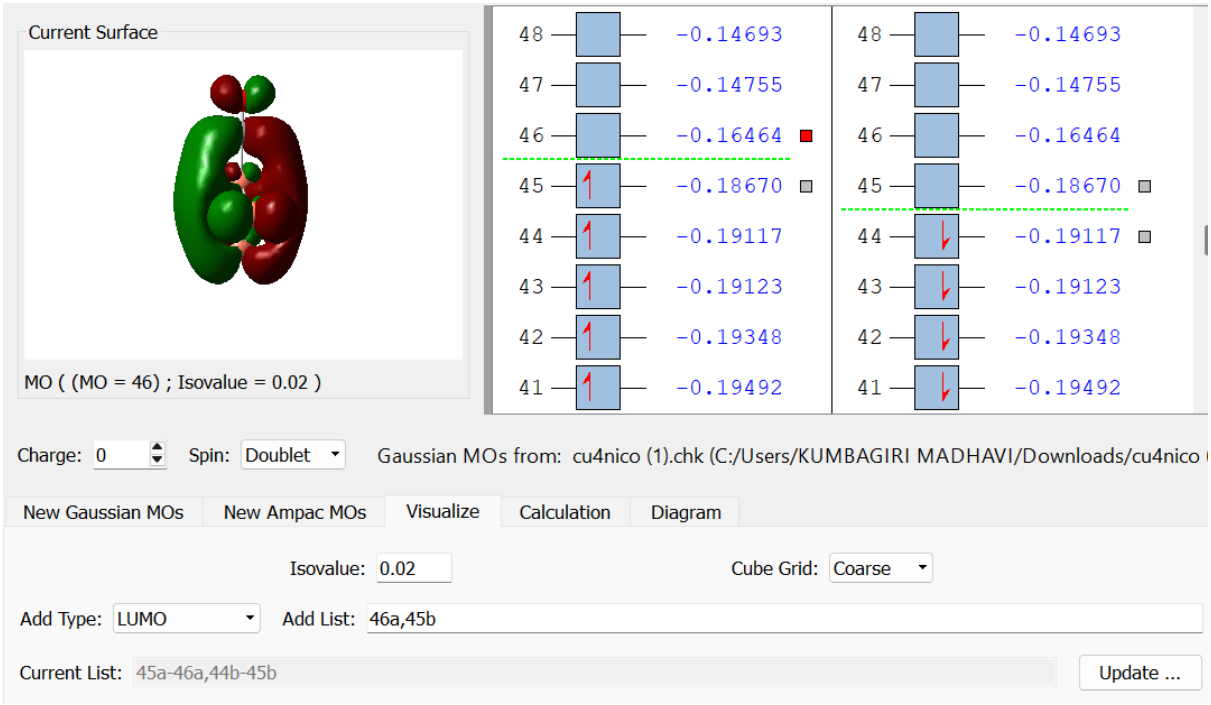

FIG 1.10 LUMO Orbital

Definition:

LUMO: Represents the lowest energy orbital that can accept electrons. It is critical for understanding the electronic structure, stability, and reactivity of a molecule.

Units:

Energy levels of the LUMO are typically expressed in electron volts (eV) or atomic units (a.u.), depending on the computational framework.

2.5.1 DFT Calculation:

Determine LUMO Energy: After performing a DFT calculation, the energy of the LUMO can be identified from the energy levels of the unoccupied Kohn-Sham orbitals.

Procedure: Solve the Kohn-Sham equations to obtain the orbital energies and identify the lowest energy orbital that is not filled with electrons.

Applications:

Chemical Reactivity: The LUMO energy is used in frontier molecular orbital theory to predict how a molecule will interact with nucleophiles (electron donors) and electrophiles (electron acceptors).

Spectroscopy: LUMO levels influence the absorption spectra and electronic transitions, including UV-V is spectroscopy.

Material Design: Important for organic electronics, where the LUMO affects the efficiency of charge transport and the interaction of materials with light or other electronic devices.

The energy difference between the HOMO (Highest Occupied Molecular Orbital) and the LUMO is known as the HOMO-LUMO gap. This gap is crucial for understanding the electronic and optical properties of a molecule or material. A larger HOMO-LUMO gap often indicates greater stability and less reactivity, while a smaller gap can imply increase reactivity and electronic activity.

The LUMO in DFT provides essential information about the lowest available energy state for electron acceptance in a molecule, which is key for understanding its electronic properties, reactivity, and potential applications in various fields of chemistry and material science.

In Density Functional Theory (DFT), the chemical potential (μ) is a measure of the change in the total energy of a system when an additional particle (typically an electron) is added, while maintaining equilibrium.

Definition:

Chemical Potential (μ): In the context of DFT, it is often associated with the energy required to add or remove an electron from the system. The chemical potential can be known by using HOMO and LUMO.

$$\mu = -\left(\frac{I}{A}\right)$$

Units:

Chemical potential is typically measured in electron volts (eV) or atomic units (a.u.).

DFT Calculation:

Determine Chemical Potential: After obtaining the total energy of the system through a DFT calculation, the chemical potential can be computed by differentiating this energy with respect to the number of electrons or by calculating the Fermi level in the context of solid-state systems.

2.7 ELECTROSTATIC POTENTIAL(ESP)

The Electrostatic Potential (ESP) is a fundamental concept in physics that describes the potential energy of a charged particle in an electric field. ESP is a crucial tool for understanding various physical phenomena, including electrostatic interactions, molecular recognition, and chemical reactivity. (16)

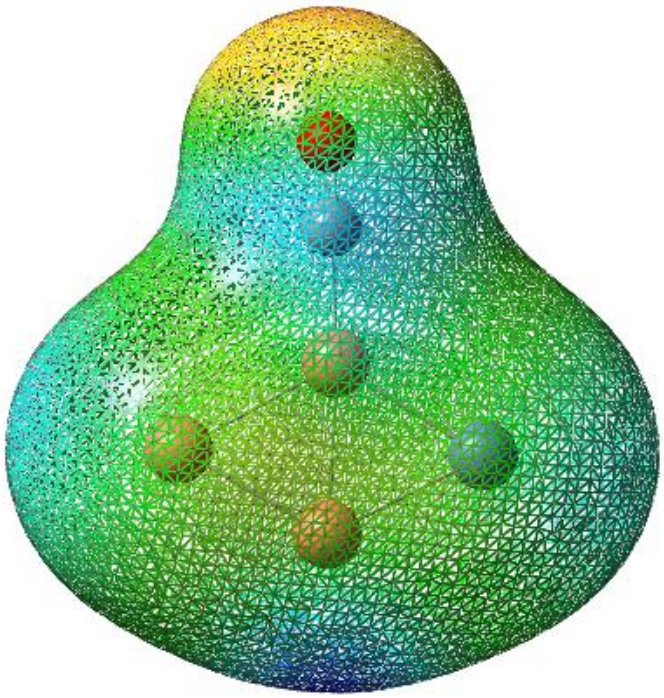

FIG 1.11 Electrostatic potential

Definition and Calculation

The ESP is defined as the potential energy of a unit charge at a point in space, typically denoted by V(r) or φ(r). It can be calculated using the Poisson equation, which relates the ESP to the charge distribution and the dielectric properties of the medium.

2.7.1 Applications

ESP has a wide range of applications in various fields, including:

- Molecular Modelling: ESP is used to study the electrostatic properties of molecules and their interactions.
- Chemical Reactivity: ESP can be used to predict the reactivity of molecules and identify potential reaction sites.
- Biological Systems: ESP is used to study the electrostatic properties of biomolecules and their interactions.

2.7.2 Visualization and Interpretation

ESP can be visualized using various techniques, including:

- Isopotential Surfaces: These surfaces represent the regions of space where the ESP has a constant value.
- ESP Maps: These maps show the distribution of ESP on a molecular surface.

2.7.3 Importance in Research

- Materials Science: ESP can be used to study the electrostatic properties of materials and their applications.
- Nanotechnology: ESP can be used to study the electrostatic properties of nanoparticles and their interactions.

2.8 Density of States

The density of states (DOS) is a fundamental concept in solid-state physics that describes the number of available states per unit energy range per unit volume in a material. It's a crucial tool for understanding various physical properties of materials, such as electrical conductivity, thermal conductivity, and optical properties. (13)

2.8.1 Definition and Calculation

The density of states is defined as the number of states per unit energy range per unit volume, typically denoted by g(E) or D(E). It's calculated using the dispersion relation, which relates the energy of a particle to its wave vector. The DOS can be calculated for electrons, photons, or phonons, and it's usually expressed as a function of energy or wave vector.

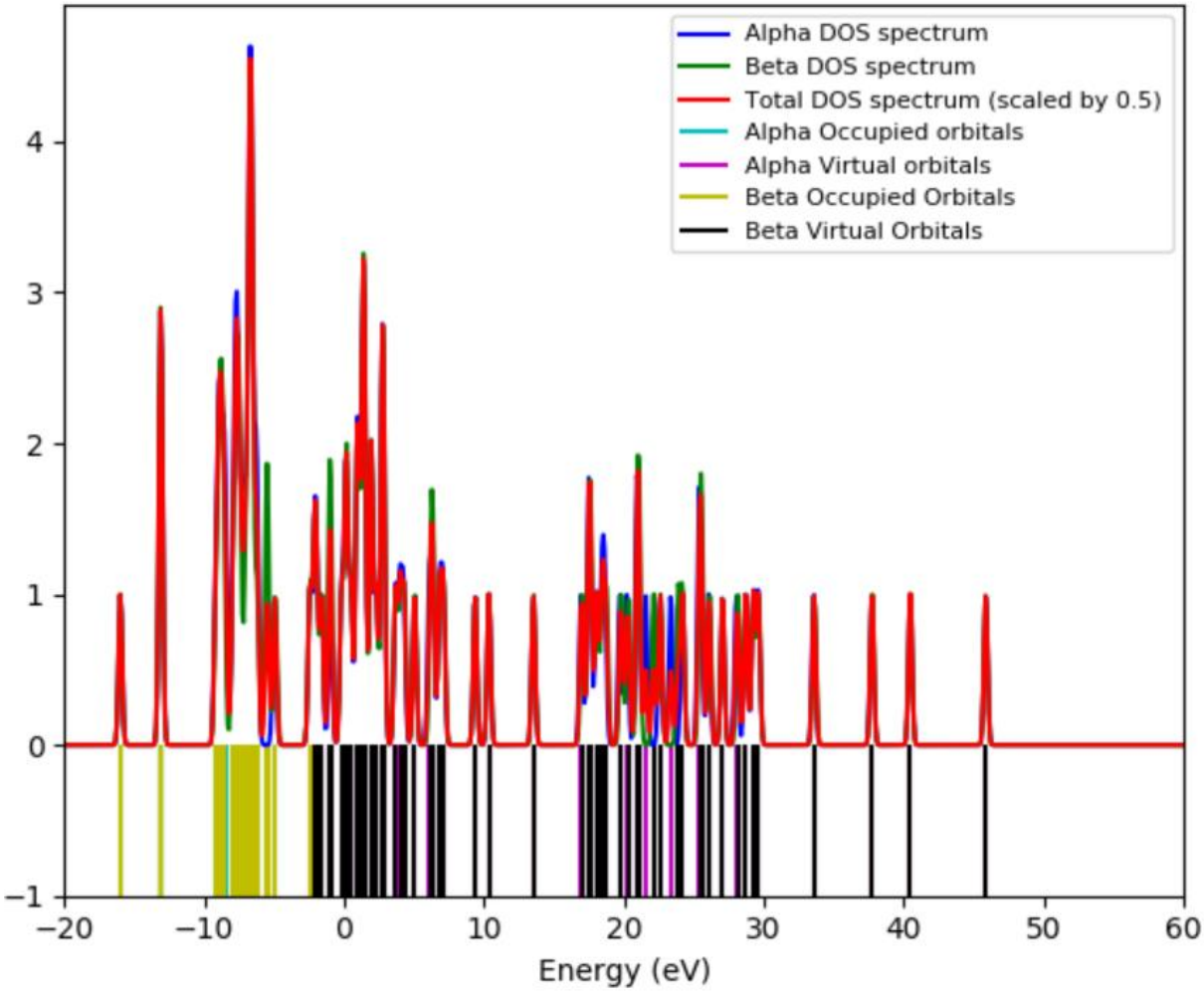

FIG 1.12 Density of states

2.8.2 Dimensionality and Density of States

The dimensionality of a system plays a significant role in determining its density of states. In general, the DOS varies with energy in different ways depending on the dimensionality of the system

- 1-Dimensional Systems: The DOS is inversely proportional to the square root of energy.
- 2-Dimensional Systems: The DOS is constant and independent of energy.
- 3-Dimensional Systems: The DOS is proportional to the square root of energy.

2.8.3 Applications

Understanding the density of states is essential for various applications, including:

- Semiconductor Physics: DOS plays a crucial role in determining the electrical conductivity of semiconductors.
- Nanotechnology: The DOS in nanoscale systems can be significantly different from that in bulk materials, leading to unique properties.
- Optics and Photonics: The DOS of photons is important for understanding the behaviour of light in various materials and structures.

The local density of states (LDOS) is a concept related to the DOS, which describes the density of states at a specific point in space. LDOS is useful for understanding the behaviour of materials at the nanoscale, where the DOS can vary significantly from point to point

2.9 Energy Gap

The energy gap, also known as the bandgap, is a fundamental concept in solid-state physics that plays a crucial role in understanding the behavior of electrons in materials. It is the energy difference between the valence band and the conduction band in a material [9]

2.9.1 Definition of Energy Gap

The energy gap is the minimum energy required to excite an electron from the valence band to the conduction band, where it can participate in electrical conduction. The size of the energy gap determines the electrical conductivity of a material.

2.9.2 Types of Energy Gaps

- Direct Bandgap: In direct bandgap materials, the valence band maximum and conduction band minimum occur at the same momentum, allowing for efficient optical transitions.
- Indirect Bandgap: In indirect bandgap materials, the valence band maximum and conduction band minimum occur at different momenta, making optical transitions less efficient.

2.9.3 Importance of Energy Gap

- Electrical Conductivity: The energy gap determines the electrical conductivity of a material, with materials having a small energy gap being more conductive.
- Optical Properties: The energy gap affects the optical properties of materials, such as absorption and emission of light.

- Device Applications: The energy gap is crucial for designing electronic and optoelectronic devices, such as transistors, solar cells, and LEDs.

2.9.4 Calculation of Energy Gap

- Density Functional Theory (DFT): DFT is a popular method for calculating the energy gap of materials.
- Many-Body Perturbation Theory (MBPT): MBPT is a more advanced method that can provide accurate calculations of energy gaps.

2.9.5 Applications

- Semiconductors: Understanding the energy gap is essential for designing semiconductor devices, such as transistors and solar cells.
- Optoelectronics: The energy gap plays a crucial role in designing optoelectronic devices, such as LEDs and lasers.
- Materials Science: The energy gap is important for understanding the properties of materials and designing new materials with specific properties.

2.10 Fermi Energy

The Fermi energy is a fundamental concept in solid-state physics that plays a crucial role in understanding the behaviour of electrons in metals and semiconductors. It is named after the Italian physicist Enrico Fermi, who made significant contributions to the development of quantum mechanics and statistical mechanics. [7-8]

Definition of Fermi Energy

The Fermi energy, also known as the Fermi level, is the energy level at which the probability of finding an electron is 50%. It is a measure of the energy of the highest occupied state in a system of fermions at absolute zero temperature.

Importance of Fermi Energy

- Electronic Properties: The Fermi energy determines the electronic properties of metals and semiconductors, such as conductivity and carrier concentration.
- Thermal Properties: The Fermi energy influences the thermal properties of materials, such as specific heat capacity and thermal conductivity.

- Optical Properties: The Fermi energy affects the optical properties of materials, such as reflectivity and absorption.

Calculation of Fermi Energy

- Free Electron Model: The free electron model is a simple model that can be used to estimate the Fermi energy of metals.
- Density Functional Theory (DFT): DFT is a more advanced method that can be used to calculate the Fermi energy of materials.

Applications

- Electronics: Understanding the Fermi energy is crucial for designing electronic devices, such as transistors and diodes.
- Materials Science: The Fermi energy plays a key role in understanding the properties of materials, such as their electrical and thermal conductivity.
- Nanotechnology: The Fermi energy is important for understanding the behaviour of nanoparticles and nanostructures.

2.11 Adsorption Energy

Adsorption energy is a fundamental concept in surface science that plays a crucial role in understanding the interaction between molecules and surfaces. It is defined as the energy change associated with the adsorption of a molecule onto a surface [10].

Definition of Adsorption Energy

The adsorption energy is a measure of the strength of the interaction between the adsorbate (the molecule being adsorbed) and the substrate (the surface). It is typically measured in units of energy per mole of adsorbate.

Importance of Adsorption Energy

- Surface Chemistry: Adsorption energy is crucial for understanding surface chemical reactions, such as catalysis and corrosion.
- Materials Science: Adsorption energy plays a key role in understanding the properties of materials, such as their surface energy and wettability.
- Nanotechnology: Adsorption energy is important for understanding the behavior of nanoparticles and nanostructures.

Calculation of Adsorption Energy

- Density Functional Theory (DFT): DFT is a popular method for calculating the adsorption energy of molecules on surfaces.
- Molecular Dynamics Simulations: Molecular dynamics simulations can be used to study the adsorption behaviour of molecules on surfaces.

Applications

- Catalysis: Understanding adsorption energy is essential for designing catalysts and optimizing catalytic reactions.
- Surface Modification: Adsorption energy plays a crucial role in surface modification techniques, such as coating and functionalization.
- Sensing and Detection: Adsorption energy is important for designing sensors and detection systems that rely on surface interactions.

2.12 INFRARED SPECTRA

Infrared (IR) spectroscopy is a powerful analytical technique used to identify and characterize molecules based on their vibrational transitions. It involves measuring the interaction between infrared light and a molecule, resulting in a unique spectrum that serves as a molecular fingerprint

Principle of IR Spectroscopy

IR spectroscopy works on the principle that molecules absorb specific frequencies of infrared radiation, causing vibrational transitions. These transitions occur when the energy of the infrared radiation matches the energy difference between the vibrational energy levels of the molecule. The resulting IR spectrum is a plot of infrared intensity versus wavelength or frequency

Interpretation of IR Spectra

IR spectra can be interpreted by analysing the peak positions, intensities, and widths. Peak positions are related to the type of bond or functional group present in the molecule, while peak intensities are related to the concentration of the molecule. The width of the peaks can provide information about the molecular environment and intermolecular interactions

Applications of IR Spectroscopy

IR spectroscopy has a wide range of applications in various fields, including:

- Material Analysis: IR spectroscopy is used to analyse the composition of materials and identify contaminants.
- Chemical Identification: IR spectroscopy can be used to identify unknown compounds and determine their molecular structure.
- Biological Analysis: IR spectroscopy is used in biomedical research to analyse biological samples and diagnose diseases.
- Environmental Monitoring: IR spectroscopy can be used to monitor environmental pollutants and detect changes in atmospheric composition.

Instrumentation

The main components of an IR spectrometer include:
- Radiation Source: A broadband emitter that produces infrared radiation.
- Sample Cells: Used to hold the sample in place during measurement.
- Monochromators: Used to select specific wavelengths of infrared radiation.
- Detectors: Used to measure the intensity of the infrared radiation.
- Recorder: Used to record the IR spectrum.

Advantages and Limitations

IR spectroscopy has several advantages, including:
- High Speed: IR spectra can be acquired quickly using Fourier transform infrared (FTIR) spectroscopy.
- High Sensitivity: IR spectroscopy can detect small amounts of sample.
- Non-Destructive: IR spectroscopy is a non-destructive technique, allowing for further analysis of the sample

2.13 HARDNESS (η)

In Density Functional Theory (DFT), hardness is a measure of a system's resistance to changes in its electronic structure, particularly in response to perturbations like chemical reactions or external fields.

$$\emptyset = \frac{I + A}{2}$$

Where I is the $-E_{HOMO}$ and A is the $-E_{LUMO}$

Chemical Hardness (η):

The Chemical Hardness is the calculated by the values of HOMO and LUMO

$$\eta = \frac{I - A}{2}$$

It quantifies how much the energy of the system changes with a small addition or removal of electrons.

Units:

Hardness is typically measured in electron volts (eV) or atomic units (a.u.).

DFT Calculation:

Approximate Method: Direct calculation of chemical hardness from DFT is not straightforward. It is often approximated using the difference between the HOMO and LUMO energies:

$$\eta = \frac{I - A}{2}$$

Kohn-Sham Orbitals: Calculate the energy levels of the HOMO and LUMO, then use these to estimate the hardness.

Applications:

Reactivity: Hardness is used to predict the stability and reactivity of chemical species. High hardness indicates a stable species that resists changes, while low hardness suggests greater reactivity.

Chemical Reactions: Helps in understanding how molecules will interact in chemical reactions, especially in terms of nucleophilic and electrophilic attacks.

Material Science: Useful for assessing the stability and hardness of materials, guiding the design of new materials with desired mechanical properties.

Relation to Other Properties:

Stability: Hardness is an indicator of a system's stability, with higher hardness correlating with increased resistance to change.

Hardness in DFT provides a measure of a system's electronic resistance to perturbations, aiding in the prediction of chemical reactivity and material stability.

In the context of density functional theory (DFT), "softness" is often discussed in terms of how a system's electronic density responds to external perturbations. Here is a summary of how softness is related to DFT, its significance in various applications, and units used in calculations:

2.14 Softness

Definition: Softness in DFT refers to the sensitivity of the electron density of a system to changes in the external potential. In a more technical sense, it can be linked to the "density response" of a system, which describes how the electron density adjusts in response to external fields or perturbations.

Physical Meaning: In practical terms, softness can indicate how easily the electronic structure of a material can be perturbed. For example, materials with high softness might exhibit significant changes in their electronic properties in response to small external influences.

$$S=\frac{1}{2\eta}$$

By knowing the value of η we can know the value of Softness.

1. Applications of Softness

Material Design: Softness helps in designing materials with specific electronic properties by understanding how their electron density will respond to external stimuli, such as applied electric fields or pressure.

2. Chemical Reactions: Softness can influence reaction mechanisms and activation energies, aiding in predicting how easily certain chemical reactions will proceed.

Spectroscopy: In spectroscopic studies, knowing the softness of a material can help interpret how the material will interact with electromagnetic radiation, impacting techniques such as photoelectron spectroscopy.

3. Calculation Units

In DFT calculations, different units and parameters are used depending on the aspect of the theory being applied

Energy Units: Typically, energy is measured in electronvolts (eV) or Hartrees (Ha). For instance, 1 eV = 27.2114 eV.

Density Units: Electron density is often expressed in units of electrons per cubic angstrom ($e/Å^3$) or electrons per cubic meter (e/m^3).

Potential Units: The external potential and response functions are usually measured in volts per angstrom (V/Å) or electronvolts (eV), depending on the context.

Response Functions: These can be expressed in various units depending on how they are defined in relation to the perturbations they are responding to.
Understanding the softness of a material in DFT requires a good grasp of these units and their implications for the material's electronic structure and properties. Each application might use specific details tailored to the system being studied, but the general principles remain consistent.

2.15 ELECTROPHILICITY (ω)

In Density Functional Theory (DFT), electrophilicity refers to a molecule's tendency to accept electrons, which is a key concept in understanding chemical reactivity and interactions. Electrophilicity is closely related to the concept of electrophiles in chemistry, which are species that seek out electron-rich regions to react.

Definition: Electrophilicity is a measure of the ability of a molecule or atom to accept electrons. It's an important concept in chemistry, particularly in understanding reaction mechanisms and predicting reactivity.

1. Electrophilicity index (ω): Developed by Parr and coworkers, this index is based on the electronic chemical potential and hardness.

$$\omega = \frac{\mu^2}{2\eta}$$

where μ is the chemical potential and η is the hardness.

Units:

The electrophilicity index is typically measured in electron volts (eV) or atomic units (a.u.), depending on the context.

DFT Calculation:

The DFT calculations are done by using the HOMO and LUMO values. It is related to the Chemical Potential

Applications:

Reactivity Predictions: Helps in predicting how molecules will react with nucleophiles. Molecules with high electrophilicity are more likely to act as electrophiles in chemical reactions.

Molecular Design: Useful in designing new molecules or materials, especially in organic synthesis, to target specific reactive sites.

Chemical Reactions: Provides insights into the reactivity and interaction of molecules in various chemical environments.

Relation to Other Properties:

Electronegativity: Electrophilicity is related to electronegativity, which is a measure of a molecule's ability to attract electrons. In general, more electrophilic species have higher electronegativity.

Reactivity: The electrophilicity index indicates how reactive a molecule might be toward nucleophiles; higher values suggest greater reactivity.

Summary:

Electrophilicity in DFT helps characterize a molecule's ability to accept electrons, which is crucial for predicting chemical reactivity and interactions. By calculating the electrophilicity index, chemists can gain insights into how a molecule might behave in chemical reactions, aiding in the design and understanding of chemical processes.

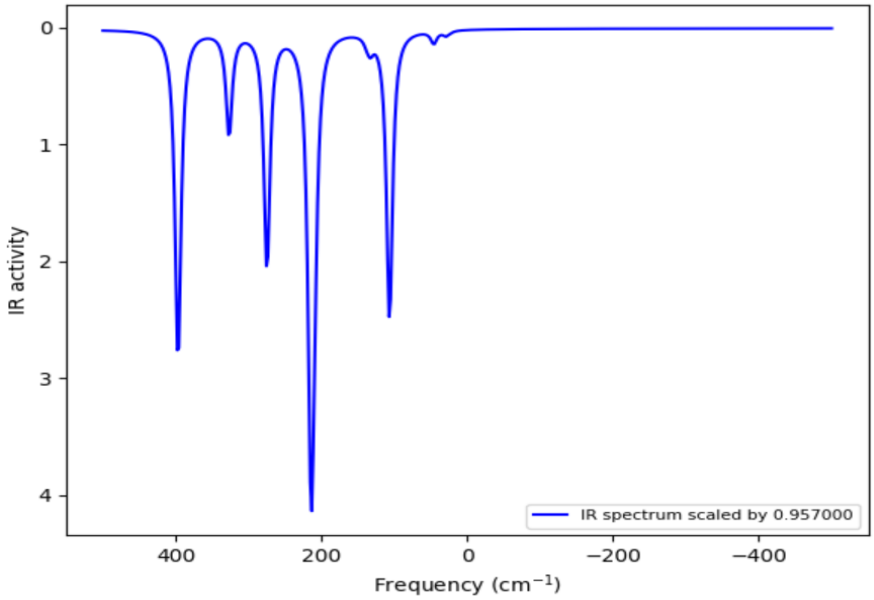

FIG 1.13 IR Spectrum

2.16 Reduced Density Gradient

The Reduced Density Gradient (RDG) is a fundamental concept in density functional theory (DFT) and computational physics. It is used to analyse and visualize the bonding and non-bonding interactions in molecules. (17)

Applications

RDG has several applications in physics and chemistry, including:

- Bonding Analysis: RDG can be used to identify and characterize bonding interactions in molecules.
- Non-Covalent Interactions: RDG can be used to study non-covalent interactions, such as van der Waals forces and hydrogen bonding.
- Molecular Structure: RDG can be used to analyze the molecular structure and identify regions of high reactivity.

Visualization

RDG can be visualized using isosurfaces, which represent the regions of space where the RDG has a certain value. These isosurfaces can be colored according to the sign of the second eigenvalue of the Hessian matrix of the electron density, allowing for the identification of different types of interactions.

Importance in Research

RDG is an important tool in research, particularly in the fields of:

- Materials Science: RDG can be used to study the bonding and non-bonding interactions in materials.
- Pharmaceuticals: RDG can be used to design and optimize pharmaceutical molecules.
- Catalysis: RDG can be used to study the bonding and reactivity of catalysts.

2.17 NATURAL BOND ORBITAL (NBO)

Natural Bond Orbital (NBO) analysis is a powerful tool in computational physics and chemistry that provides insight into the electronic structure and bonding of molecules. (18)

What is NBO Analysis?

NBO analysis is a method that transforms the molecular orbitals of a molecule into a set of localized orbitals that correspond to chemical bonds, lone pairs, and other electronic features.

Applications of NBO Analysis

NBO analysis has several applications in physics and chemistry, including:

- Bonding Analysis: NBO analysis can be used to study the nature of chemical bonds and identify the type of bonding (e.g., σ, π, or δ) between atoms.
- Charge Transfer: NBO analysis can be used to study charge transfer between molecules or within a molecule.
- Molecular Structure: NBO analysis can be used to analyze the molecular structure and identify regions of high reactivity.

Key Features of NBO Analysis

- Localized Orbitals: NBO analysis provides a set of localized orbitals that correspond to chemical bonds, lone pairs, and other electronic features.
- Natural Population Analysis: NBO analysis provides a natural population analysis (NPA) of the molecular orbitals, which can be used to calculate atomic charges and orbital occupancies.

Importance in Research

NBO's importance in research is significant, particularly in the fields of:

- Materials Science: NBO analysis can be used to study the bonding and reactivity of materials.
- Pharmaceuticals: NBO analysis can be used to design and optimize pharmaceutical molecules.
- Catalysis: NBO analysis can be used to study the bonding and reactivity of catalysts.

CHAPTER -III

Results and Discussion

3.1 Structural optimization and stability of pristine nanoclusters.

The Fig. 1 represents the optimized structure of both Cu_4 and Cu_6 clusters. The Cu-Cu bond lengths for the Cu_4 and Cu_6 clusters are 2.45 Å and 2.39 Å, respectively, and these values are consistent with previous literature. In the Cu_4 cluster, the arrangement of Cu atoms forms a parallelogram shape with a diagonal bond between the two middle Cu atoms. In contrast, the Cu_6 clusters exhibit a triangular arrangement of Cu atoms.

Furthermore, the Cu_4 clusters have a HOMO-LUMO gap (E_g) of 1.89 eV, as determined by equation (1), while the Cu_6 clusters show a bandgap of 3.26 eV. Additionally, the corresponding electronic parameters, such as E_{HOMO}, E_{LUMO}, E_g, and E_F, are provided in Table 1. To assess structural stability, we calculated the binding energy (E_B) using the following formula:

$$E_B = \frac{E(Cu_4/Cu_6\ cluster) - n \times E(Cu)}{n} \qquad \ldots\ldots\ldots\ldots\ldots\ldots\ldots (3)$$

Where, E(Cu_4/Cu_6 cluster) and E (Cu) are the total energy of pristine Cu-cluster and isolated Cu atom, respectively and n is the number of Cu atoms present in Cluster.

The Cu_4 cluster exhibits a binding energy of -3.39 eV, while the Cu_6 cluster has a slightly more negative E_B of -3.69 eV. This negative formation energy implies that both clusters are structurally stable. A more negative formation energy value generally indicates a stronger stability of the cluster. To assess the dynamical stability of the clusters, we performed an analysis of the IR spectra.

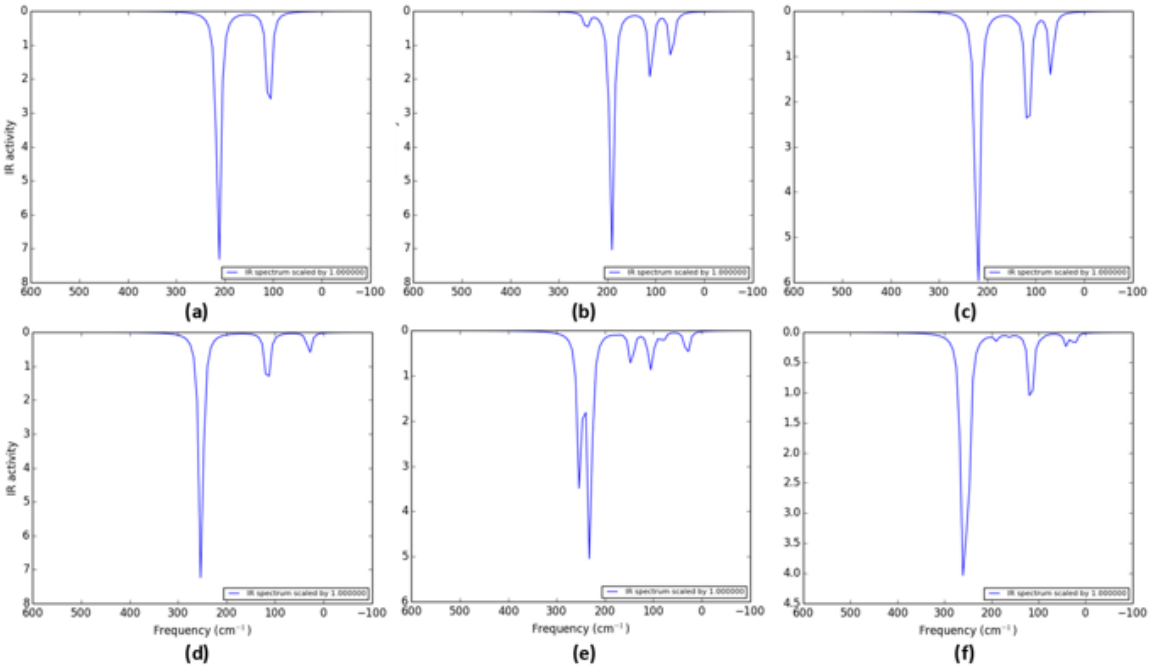

FIG 1.13 IR of (a) Cu_4, (b) Cu_3Ag, (c) Cu_3Ni, (d) Cu_6, (e) Cu_3Ag, (f) Cu_5Ni Nanoclusters

The IR spectra provide insight into the stability through the vibrational frequency mode present in the system. The absence of imaginary frequencies (i.e., all positive frequencies) suggests the dynamical stability of the structures. Upon analysing the IR spectra of the Cu_4 cluster, we observed a higher intensity peak around a frequency of 200 cm^{-1}, with all positive frequencies indicating dynamical stability. On the other hand, the IR spectra of the Cu_6 cluster revealed two minor peaks and major peaks in the range of 200-300 cm^{-1}, also with all positive frequencies, indicating stability.

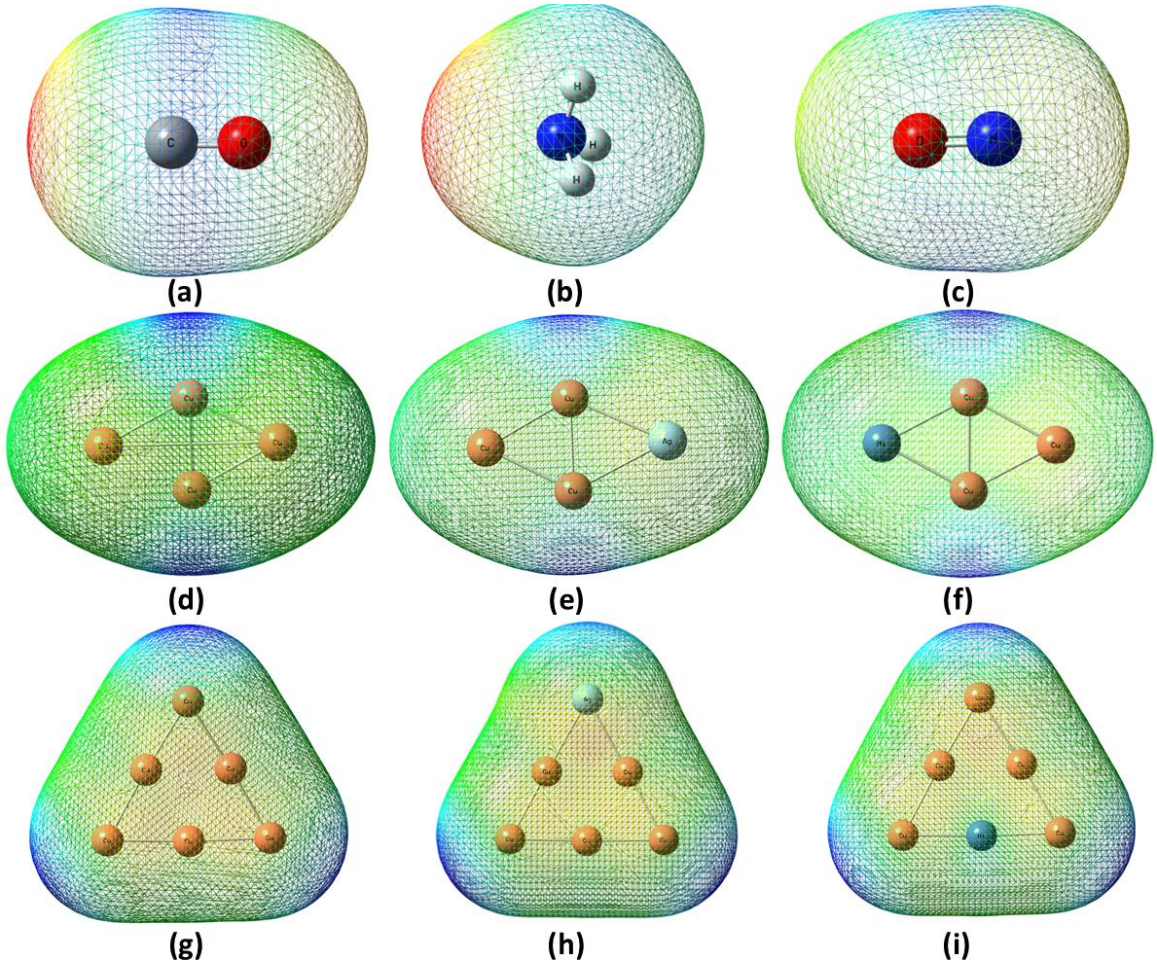

FIG 1.14 ESP Mapping of (a)CO, (b)NH_3, (c)NO Gas and (d) Cu_4, (e) Cu_3Ag, (f) Cu_3Ni, (g)Cu_6, (h) Cu_5Ag, (i) Cu_5Ni Nanocluster

3.1.2 DOS and Electronic parameters

The Density of States (DOS) spectra is used to understand the distribution of orbital electrons. The DOS spectra for pristine Cu_4 and Cu_6 clusters can be found in Fig. S2 (a and d). Electronic parameters such as E_{HOMO}, E_{LUMO}, E_g, change in E_g (ΔE_g), and E_F are listed in Table 1. For the pristine Cu_4 cluster, E_{HOMO} and E_{LUMO} are -4.75 eV and -2.85 eV, respectively, resulting in a bandgap (E_g) of 1.89 eV. For the Cu_6 cluster, the E_{HOMO} and E_{LUMO} values are -5.50 eV and -2.24 eV, respectively, resulting in a bandgap of 3.26 eV.

The distribution of HOMO electron density (HOMO-ED) and LUMO electron density (LUMO-ED) for the pristine clusters can be seen in Fig. 1 (a and

d, respectively). The HOMO-ED and LUMO-ED for the Cu_4 cluster are evenly distributed over the Cu atoms. However, for the Cu_6 cluster, the HOMO-ED is primarily located near the edge atoms, while the LUMO-ED is evenly distributed over all Cu atoms.

In our investigation, we delved into the Mulliken charge distribution across Cu clusters. The Mulliken charge values are suggested by colour, with red depicted for negative charge values and green for positive charges. Darker colour represents more concentrated charge values The pristine Cu_4 and Cu_6 clusters showcased a dipole moment of 0.00 Debye, indicating equitable interactions among the Cu atoms. Furthermore, we analysed the molecular electrostatic potential (MEP) surfaces, presented in Fig. 3, which divulge crucial information regarding interacting potential. The blue, red, and green regions correspond to positive potential, negative potential, and neutral potential, respectively. Fig. 3 (a to c) illustrates the MEP of toxic gas molecules (CO, NO, and NH_3). Upon examination, the MEP of the pristine Cu_4 and Cu_6 clusters unveiled a positive potential region (denoted by blue colour) proximate to the edge Cu atoms (Fig. 3(d and g)).

3.2 Structural optimization and stability of Transition Metals

In order to improve the adsorption properties of pure Cu clusters, we decorated them with transition-metal (TM) atoms like nickel (Ni) and silver (Ag). After optimizing the structure with TMs at different sites, we found that the most favourable optimization case is shown in Fig. 1(b,c,e,f). When Cu_4 is substitutionally doped with Ag, the bond length changes to 2.67 Å (Cu-Ag) from 2.45 Å (Cu-Cu). However, there are only small changes in the bond length of Ni-decorated Cu_4 (2.40 Å from 2.45 Å). Similarly, the Cu_4 cluster has a bond length of 2.59 Å (Cu-Ag) and 2.40 Å (Cu-Ni) after being decorated with Ag and Ni atoms respectively, compared to 2.39 Å (Cu-Cu) without decoration and are shown in table 1.

System	E_{LUMO} (eV)	E_{HOMO} (eV)	E_g (eV)	E_F (eV)	E_B (eV/atom)
Cu_4	-2.854	-4.752	1.897	-3.803	-3.385
Cu_3Ag	-2.857	-4.768	1.911	-3.812	-2.832
Cu_3Ni	-2.806 $^{\alpha}$	-4.796 $^{\alpha}$	1.989 $^{\alpha}$	-3.801 $^{\alpha}$	-3.265
	-2.786 $^{\beta}$	-4.732 $^{\beta}$	1.947 $^{\beta}$	-3.759 $^{\beta}$	
Cu_6	-2.242	-5.503	3.261	-3.873	-3.693
Cu_5Ag	-2.341	-5.461	3.120	-3.901	-3.316
Cu_5Ni	-2.229 $^{\alpha}$	-5.449 $^{\alpha}$	3.219 $^{\alpha}$	-3.839 $^{\alpha}$	-3.616

Table 1: Calculated Values of LUMO Energy (E_{LUMO}), HOMO Energy (E_{HOMO}), Fermi Level (E_F), HOMO−LUMO Gap (E_g) and Binding Energy (E_B) of Cu_4, Cu_3Ag, Cu_3Ni, Cu_6, Cu_5Ag, and Cu_5Ni nanoclusters

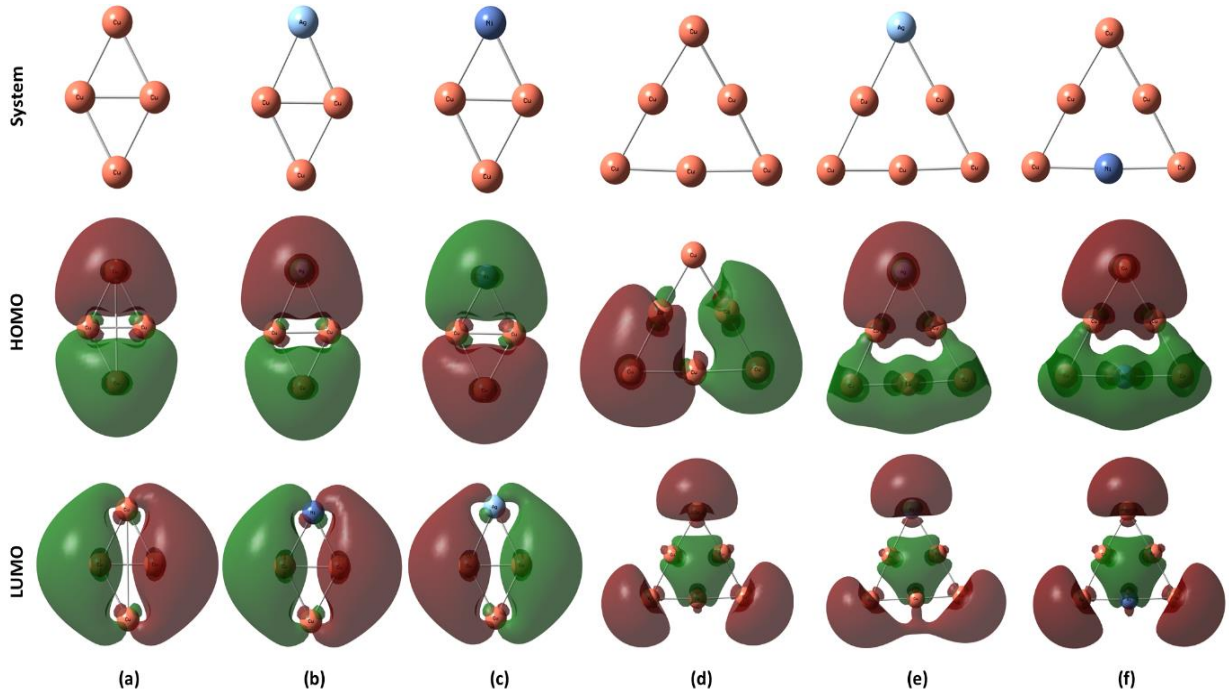

FIG 1.15 HOMO and LUMO of Nanoclusters

To assess structural stability, the IR spectra were analysed for Ag and Ni decorated Cu_4 and Cu_6 clusters. The results showed positive frequency across the entire frequency range (absence of imaginary frequency), indicating structural dynamical stability of the structures (Fig. 2 (b,c,e,f)). **Binding Energy**

Furthermore, the binding energy (E_B) for Ag and Ni decorated Cu clusters was calculated using Equation (4) given below:

$$E_B = \frac{E\ (Cu_nTM)\ -\ [n\ \times\ E(Cu) + \mathrm{E(TM)}]}{n+1} \qquad \ldots\ldots\ldots\ldots (4)$$

Where, E (Cu_n) and E (Cu) are the total energy of pristine Cu-cluster and isolated Cu atom, and E(TM) energy of transition metal atoms (Ag and Ni), respectively and n is the number of Cu atoms present in Cluster while m is a number of TM atoms present in the cluster.

The E_B for Cu_4 cluster after decorating with Ag and Ni are -2.82 eV and -3.26 eV, respectively (calculated using equation 4). Meanwhile, for the Cu_6 cluster

it is -3.32 eV and -3.62 eV for Ag and Ni decorated Cu clusters, respectively. The negative E_B indicates favourable interactions between TM atoms and Cu clusters.

3.2.1 DOS and Electronic Parameters of doped nanoclusters

The introduction of Ag and Ni atoms, which are transition metals, has a significant impact on the electronic density distribution and bandgap of Cu clusters. In Fig. S2 (b,c,e,f), the density of states (DOS) spectra of Cu clusters after being decorated with Ag and Ni atoms are illustrated. When interacting with Ni atoms, the two spin configurations, up-spin (α) and down-spin (β), result in changes in the orbitals, thus affecting the Cu atom. For the Ag-decorated Cu_4 (Cu_3Ag) cluster, the E_{HOMO} and E_{LUMO} values are -4.76 eV and -2.85 eV, respectively, with a bandgap (E_g) of 1.91 eV. In the case of Ni-decorated Cu_4 (Cu_3Ni), the α-configuration shows E_g values of 1.99eV, with E_{HOMO} and E_{LUMO} of -4.79 eV and -2.80 eV, while the β configuration exhibits E_{HOMO} and E_{LUMO} values of -4.73 eV and -2.78 eV, resulting in an E_g of 1.95 eV.

The Ag-decorated Cu_6 (Cu_5Ag) cluster shows E_{HOMO} and E_{LUMO} values of -5.46 eV and -2.34 eV, respectively, resulting in an E_g of 3.12 eV. Meanwhile, Ni-decorated Cu_6 (Cu_5Ni) indicates E_g values of 3.22 eV with E_{HOMO} and E_{LUMO} of -5.44 eV and -2.23 eV, respectively, for the α-configuration. For the β configuration, it has E_{HOMO} and E_{LUMO} values of -5.21 eV and -2.22 eV, resulting in an E_g of 2.99 eV. These changes in HOMO and LUMO energy support the alterations observed in the DOS spectra, indicating a significant interaction between the transition metals (Ag and Ni) and the Cu clusters.

For more detailed information, the electronic parameters such as E_{HOMO}, E_{LUMO}, E_g, change in E_g (ΔE), and E_F, are provided in Table 1. Additionally, the HOMO electron density (HOMO-ED) and LUMO electron density (LUMO-ED) of Cu clusters after interacting with transition metals (Ag and Ni) are represented in Fig. 1 (b,c,e,f). Interestingly, the HOMO-ED and LUMO-ED of the TMs

decorated Cu_4 clusters (Cu_3Ag and Cu_3Ni) are evenly distributed over all Cu atoms, whereas changes are observed in the HOMO-ED of the TMs decorated Cu_6 cluster.

To get insight into the interaction between TMs (Ag and Ni) and Cu clusters, we have observed the charge transfer between them. Fig. S3 (b and c) shows the Mulliken charge distribution of Cu_3Ag and Cu_3Ni.The total charge on both decorated clusters is 0.00e but the charge transfer between Cu atom and TMs atoms takes place which indicates interactions between Cu clusters and TMs (Ag and Ni) atoms.

Mulliken charges

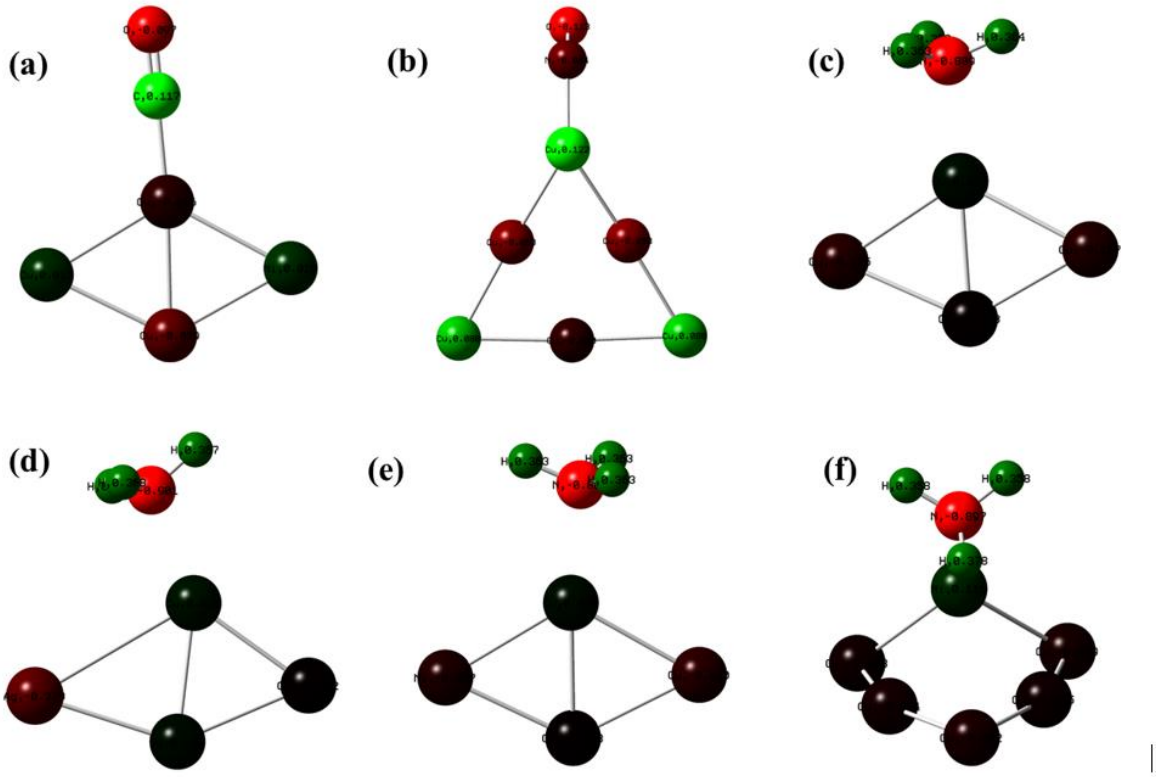

FIG 1.17 Mullikan Charges Analysis of Complex (a) CO/Cu_3Ni, (b) NO/Cu_6, (c)NH_3/Cu_4, (d) NH_3/Cu_3Ag, (e) NH_3/Cu_3Ni, (f) NH_3/Cu_5Ni

The detailed analysis of Mulliken charge distribution and DOS spectra provides us with a view of the interaction between Cu cluster and TM atoms, Zakir Ullah et. al does a similar discussion,to get insight into the adsorption of 5-Fluoro-2-Oxo-1H-Pyrazine-3-Carboxamide (OPC) over different nanocages. However, the dipole moments of Cu_3Ag and Cu_3Ni clusters are 0.58 Debye and 0.16 Debye, respectively. Furthermore, the Mulliken charge distribution of Cu_5Ag and Cu_5Ni is 0.00e, although there is a charge transfer between Cu atom and TMs atoms take place which indicates interactions between Cu clusters and TMs (Ag and Ni) atoms (Fig. S3 (e and f)). Meanwhile, the dipole moment of Cu_5Ag and Cu_5Ni is 0.07 Debye and 0.27 Debye, which supports stronger interactions between Ni atom and

Cu cluster. The MEP of the doped Cu cluster results in a continuous distribution of green and blue regions over the surfaces (Fig. 3 (e,f,h, i))

3.3 Adsorption of toxic gas molecules (CO, NO, and NH_3) on pristine Cu_4,Cu_6 clusters and TM-decorated clusters

3.3.1 Adsorption of toxic gases

Fig. 4 indicates the optimised geometry of toxic gas molecules (CO, NO, and NH_3) adsorbed pristine and TMs decorated Cu clusters. To assess adsorption interaction, firstly we have calculated adsorption energy (E_{ad}) of a system using given equation below:

E_{ad} = [E (Cu_4/Cu_6 cluster + gas molecules)) − [E (Cu_4/Cu_6 cluster) + E (gas molecules)]___[5]

Where E (Cu_4/Cu_6 cluster + gas molecules) is the total energy of clusters after adsorption of toxic gas molecules, E (Cu_4/Cu_6 cluster), and E (gas molecules) are the total energy of Cu clusters and toxic gas molecules respectively.

The optimized geometry of pristine and transition metal (TM) decorated Cu clusters was examined after the adsorption of toxic gases (CO, NO, and NH_3) in Fig. 4 (a to f). The bond length of Cu-Ni increased to 2.47 Å from 2.45 Å following NH_3 adsorption, indicating a stronger interaction. Similarly, the bond length of Cu-Ag in the Cu_3Ag cluster increased to 3.14 Å from 2.67 Å, signalling a stronger interaction, whereas the Cu_3Ni cluster showed a small elongation in bond length to 2.50 Å from 2.45 Å after NH_3 adsorption. Additionally, the Cu_5Ni cluster exhibited changes in bond length to 2.44 Å after NH_3 adsorption from 2.40 Å before adsorption.

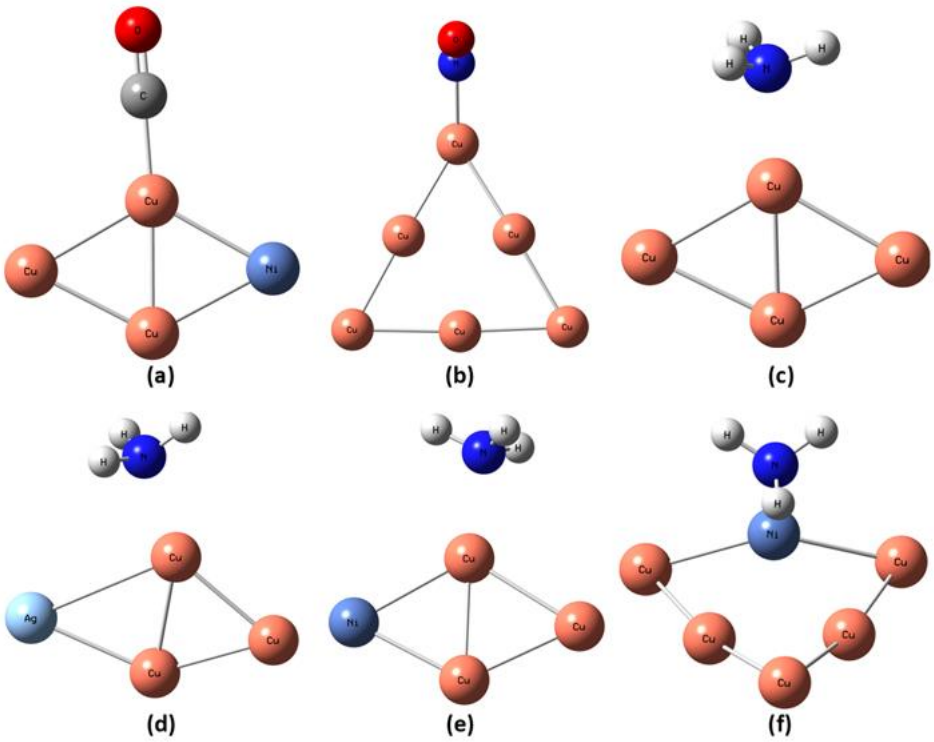

FIG 1.17 Optimised Geometry of (a) CO/Cu_3Ni , (b) NO/Cu_6, (c)NH_3/Cu_4, (d) NH_3/Cu_3Ag, (e) NH_3/Cu_3Ni , (f) NH_3/Cu_5Ni

These elongations in bond length after adsorption support the corresponding favourable interactions and adsorption energy values.

Complex	E_{LUMO} (eV)	E_{HOMO} (eV)	E_G (eV)	E_f (eV)	E_{ad} (eV)	E_{FR} (%)	E_{GR} (%)	d (Å)
CO/Cu4	-2.45	-4.96	2.51	-3.71	-0.601	-2.41	32.22	1.869
CO/Cu3Ag	-2.48	-4.97	2.49	-3.72	-0.402	-2.33	30.322	1.872
CO/Cu3Ni α	-2.44 α	-4.98 α	2.54 α	-3.71 α	-0.559 α	-2.30 α	27.56 α	1.870 α
CO/Cu3Ni β	-2.44 β	-4.92 β	2.47 β	-3.68 β	--	-2.06 β	27.22 β	--
NO/Cu4	-3.50	-5.30	1.79	-4.40	-0.798	15.80	-5.20	1.850
NO/Cu3Ag	-3.53	-5.29	1.76	-4.41	-0.773	15.77	-7.48	1.857
NO/Cu6	-3.78	-5.69	1.91	-4.74	-0.205	22.40	-41.38	1.934
NH3/Cu4	-1.75	-4.18	2.43	-2.96	-1.08	-21.99	28.26	2.049
NH3/Cu3Ag	-1.76	-4.26	2.51	-3.01	-1.11	-20.99	31.11	2.042
NH3/Cu3Ni α	-1.74 α	-4.21 α	2.47 α	-2.97 α	-1.02 α	-21.73 α	24.19 α	2.053 α
NH3/Cu3Ni β	-1.73 β	-4.14 β	2.40 β	-2.94 β	--	-21.90 β	23.41 β	--
NH3/Cu6	-1.61	-4.66	3.06	-3.13	-0.724	-19.04	-6.191	2.09
NH3/Cu5Ni α	-1.95 α	-5.03 α	3.08 α	-3.49 α	-0.893 α	-9.062 α	-4.21 α	2.078 α
NH3/Cu5Ni β	-1.95 β	-4.79 β	2.84 β	-3.37 β	--	-9.36 β	-4.88 β	--

Table 2: Calculated Value of Adsorption LUMO Energy (E_{LUMO}), HOMO Energy (E_{HOMO}), HOMO−LUMO Gap (E_g), Fermi Level (E_F), Adsorption Energy (E_{ad}), Relative Change in E_F (ΔE_{FR}), Relative Change in E_g (ΔE_{GR}), and Adsorption Distance (d) of CO, NO and NH_3 adsorb over Cu_4, Cu_3Ag, Cu_3Ni, Cu_6, Cu_5Ag, and Cu_5Ni

The E_{ad} values of CO gas molecule over the surface of pristine Cu_4, Cu_3Ag, and Cu_3Ni clusters were -0.60 eV, -0.40 eV, and -0.56 eV, respectively, indicating optimal interactions of CO with pristine Cu_4 and Cu_3Ni clusters and weaker physisorption with Cu_3Ag cluster. Notably, NO gas molecules showed significant interactions with pristine Cu_4, Cu_6, and Cu_3Ag clusters with E_{ad} values of -0.79 eV, -0.21 eV, and -0.77 eV, respectively, indicating distinct interaction strengths. Finally, NH_3 gas adsorption resulted in E_{ad} values of -1.08 eV, -1.11 eV, -1.02 eV, -0.72 eV, and -0.89 eV for pristine Cu_4, Cu_3Ag, Cu_3Ni, pristine Cu_6, and Cu_5Ni clusters, signifying varying interaction strengths and types.

3.3.2 DOS and Electronic Parameters with gases

The density of states (DOS) spectra provides valuable insights into the interactions of toxic gas molecules (CO, NO, and NH_3) with Cu clusters. In Fig. 6, you can find the DOS spectra of gas-adsorbed pristine and transition metal (TM)-decorated Cu clusters. The DOS spectra of CO-adsorbed Ni-Cu_3 clusters are presented in both α and β configurations, distinguished by different coloured lines in Fig. 5(a). Changes in occupied orbitals indicate support for the adsorption of toxic gas molecules. Additionally, the DOS spectra of pristine Cu_6 after NO adsorption are divided into up-spin and down-spin configurations, showing minimal changes in molecular orbits, suggesting a weak interaction between the two (Fig. 5(b)). Moreover, substantial changes were observed in the DOS spectra of the pristine Cu_4 cluster after interacting with NH_3 (Fig. 5(c)).

Furthermore, the adsorption of NH_3 molecules over the surfaces of Cu_3Ag and Cu_3Ni clusters results in a redistribution of molecular orbits in DOS spectra, indicating stronger interactions (Fig. 5(d, e)). Lastly, Fig. 5(f) displays the DOS spectra of Cu_5Ni after NH_3 molecule adsorption, revealing significant changes in orbital distribution that support optimal interaction between NH_3 and the Cu_5Ni cluster. The parameters as E_{HOMO}, E_{LUMO}, E_g, change in E_g (ΔE), and E_F, are given

in Table 2. The significant changes in the value of E_{HOMO} and E_{LUMO} are observed for NH_3 adsorbed pristine Cu_4, Cu_3Ni, and Cu_3Ag clusters.

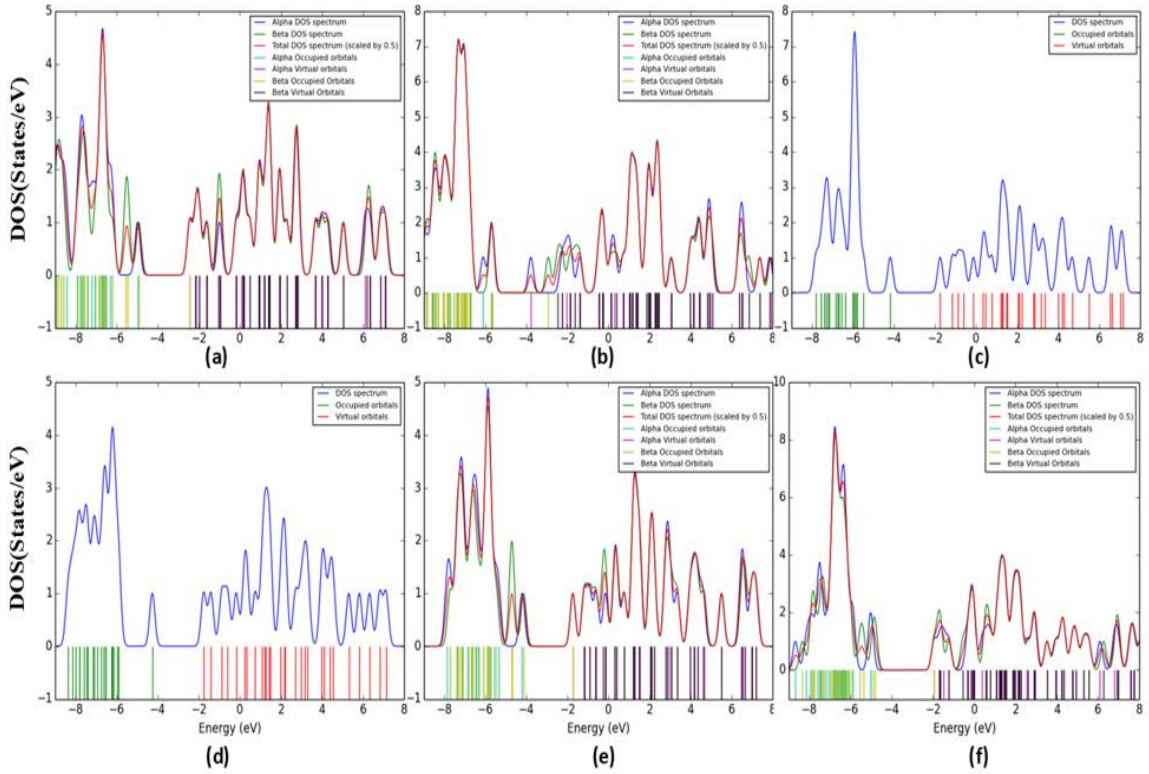

FIG 1.18 DOS Complex of (a) CO/Cu_3Ni , (b) NO/Cu_6, (c)NH_3/Cu_4, (d) NH_3/Cu_3Ag, (e) NH_3/Cu_3Ni , (f) NH_3/Cu_5Ni Nanoclusters

In the case of NH_3 adsorbed Cu_4 cluster, the E_{HOMO} and E_{LUMO} are -4.18 eV and -1.75 eV resulting in 2.43 eV of E_g while, 2.51 eV of E_g is observed with E_{HOMO} and E_{LUMO} as -4.26 eV and -1.76 eV for NH_3 absorbed Cu_3Ag. Furthermore, for NH_3 absorbed Cu_3Ni cluster, the E_{HOMO} and E_{LUMO} are -4.21 eV and -1.74 eV with E_g of 2.47 eV for spin-up configuration meanwhile, for spin-down configuration it indicates E_{HOMO} and E_{LUMO} as -4.14 eV and -1.73 eV resulting in E_g of 2.40 eV, respectively. The pristine Cu_6 and Ni-Cu_5 have optimal interactions with NH_3 molecules indicating 3.06 eV (E_{HOMO} and E_{LUMO} are -4.66 eV and -1.61 eV) and 3.08 eV for spin-up and 2.84 eV for spin-down configurations, values of E_g.

The Fig. 7 provides HOMO-ED and LUMO-ED of CO adsorbed Cu_3Ni, NO adsorbed pristine Cu_6, and NH_3 adsorbed pristine Cu_4 with NH_3 adsorbed

Cu_3Ni, Cu_5Ni, and Cu_3Ag. As indicated in Fig. 7(a), the HOMO-ED is equally distributed and LUMO-ED is entirely towards CO molecules for CO adsorbed Cu_3Ni. In the case of NO adsorbed pristine Cu_6, there are no significant changes in the distribution of HOMO-ED and LUMO-ED, indicating weak interactions (Fig. 7(b)). The Fig. 7(c) indicates equal redistribution of HOMO-ED and LUMO-ED while, LUMO-ED is entirely distributed in two positive and negative parts for NH_3 adsorbed pristine Cu_4 cluster.

However, significant changes are observed in HOMO-ED and LUMO-ED of NH_3 adsorbed Cu_3Ni, Cu_5Ni, and Cu_3Ag clusters which supports its adsorption energy values and indicates stronger interaction of NH_3 with clusters.

The Mulliken charge transfer analysis provides a better understanding of the interaction between toxic gas molecules (CO, NO, and NH_3) and clusters. Fig. 6(a to f) illustrates the Mulliken charge transfer of NH_3 adsorbed Cu_4, Cu_3Ni, and Cu_3Ag clusters (Fig. 6(a, b, and c, respectively)). Additionally, Fig. 6(d) depicts the same for CO adsorbed Cu_4.

The Mulliken charge analysis of NO adsorbed Cu_6 and NH_3 adsorbed Cu_5Ni clusters can be found in Fig. 6(e and f). There is a notable charge transfer, especially in the case of NH_3 adsorbed Cu_4 cluster (-0.73e, losing its charge to NH_3 molecules) and Cu_3Ag clusters (-0.07e). It should be noted that before adsorption, the total Mulliken charge of Cu_4 and Cu_3Ag clusters was 0.00e. However, the clusters after gas adsorption show a total 0.00e value of Mulliken charge, but there is a significant charge transfer between gas molecules and clusters over individual atoms of clusters. The dipole moment values provide valuable information about changes in properties after and before interactions. The total dipole moment of pristine Cu_4 was 0.00 Debye, and after interactions with NH_3, it becomes 5.23 Debye. Furthermore, the dipole moment of Cu_3Ag becomes 5.50 Debye from 0.58 Debye after adsorption of the NH_3 gas molecule. The charge transfer and changes in dipole moment values indicate significant interactions between clusters and toxic gas molecules.

3.3.3 The Reduced Density Gradient analysis

A Reduced Density Gradient (RDG) plot can be helpful for evaluating and characterizing a weak or strong interaction as well as for evaluating its attraction or repulsion[50]. The RDG mainly depends on electronic density (ρ), deliberated using the following relation (equation 6);

$$RDG = \frac{1}{2(3\pi^2)^{1/3}} \frac{|\nabla\rho|}{\rho^{4/3}} \quad \text{.....(6)}$$

The negative value of sign (λ2) indicates attractive interaction about charge density (ρ), and the positive value, indicates repulsive interaction about ρ.

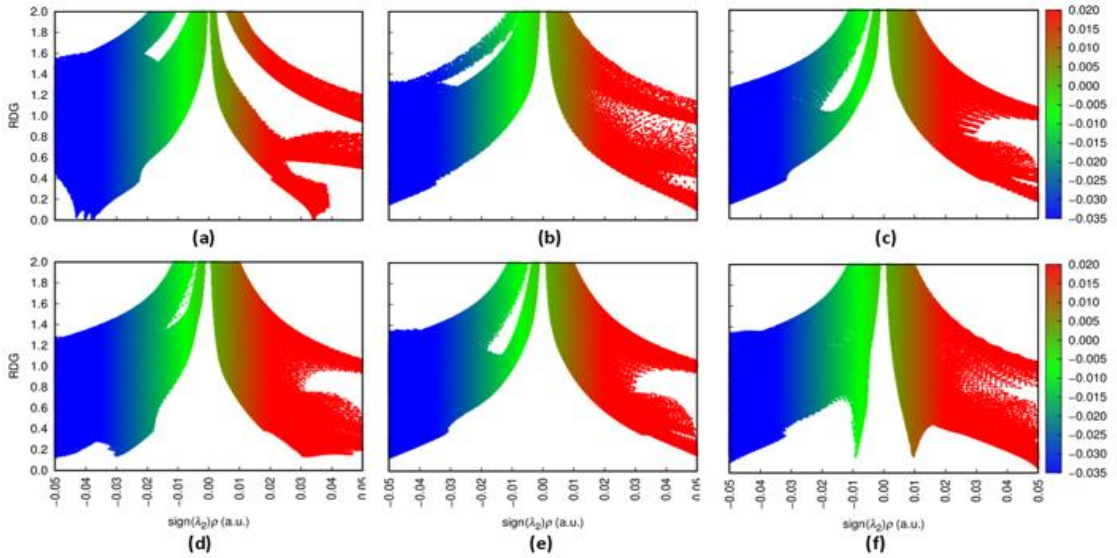

FIG 1.19 The reduced density gradient (RDG) scatter plots of (a) CO/Cu_3Ni, (b) NO/Cu_6, (c)NH_3/Cu_4, (d) NH_3/Cu_3Ag, (e) NH_3/Cu_3Ni, (f) NH_3/Cu_5Ni Complex

Interactions are governed by vdW forces when the charge density is zero (ρ = 0). Positive and negative values correspond to the strength of attraction and repulsion, respectively [51].

3.3.4 Natural Bond Orbitals analysis

In order to determine the second order perturbation energy E^2 we have performed NBO calculation and calculated the natural bond orbitals using B3LYP and Grimme's-D3 method by utilizing LanL2DZ basis sets [52][53]. Second order

perturbation energy gives the information about the interaction between the donor and acceptor atoms using the equation 7 [54].

$$E^{(2)} = \frac{F^2(ij)}{Ei - Ej} \quad \text{.....(7)}$$

Where $E^{(2)}$ is second order perturbation energy.

Table 3 represents the values of second-order perturbation energy correspond to acceptor and donors. It is clearly seen from the values that the $E^{(2)}$ value for NH_3 adsorption over Cu_3Ag is 26.68 kcal/mol which is larger as compared to other gas adsorbed nanoclusters then in Cu_3Ni and Cu_4 and then remaining are in decreasing order.

Complex	Donor	Acceptor	$E^{(2)}$ (kcal/mol)
CO/Cu_3Ni	LP*(Cu2)	BD*(C5-O6)	4.05
NO/Cu_6	LP(Cu2)	BD*(N7-O8)	2.74
NH_3/Cu_4	LP(N5)	LP*(Cu3)	11.94
NH_3/Cu_3Ag	LP(N5)	LP*(Cu2)	26.68
NH_3/Cu_3Ni	LP(N5)	LP*(Cu2)	15.75
NH_3/Cu_5Ni	BD(N7-H8)	LP*(Ni6)	4.97

Table 3: NBO Second-Order Perturbation Energy ($E^{(2)}$, kcal/mol) Corresponds to the Charge Transfer between the CO,NO and NH_3 gases and Cu_4, Cu_3Ag, Cu_3Ni, Cu_6, Cu_5Ag, and Cu_5Ni nanoclusters.

This indicates that the interaction of NH_3 is higher over Cu_3Ag, Cu_3Ni and Cu_4. However, interaction between remaining nanoclusters is comparatively less which is in accordance with adsorption energy [55]. This trend matches with the value of adsorption energy for all six complexes.

3.3.5 Sensing response

Sensing property or more precisely we can say sensing response plays important role in any study regarding gas sensing or biosensing. It is mainly due to the variation in the bandgap from the system to the complex after the adsorption occurs. the variation in bandgap is directly related to sensing response [55]. The Conductivity and resistivity relations with the sensing response are as following [56]:

$S = (\rho_2 - \rho_1)/\rho_1$ ..... (8)

$S = (\sigma_1/\sigma_2) - 1$ ..... (9)

Where, ρ_2 & ρ_1 and σ_1 & σ_2 are resistivity and conductivities of complex and system respectively. There is also equation (10)[57], which adds more detail and relates the band gap E_g and conductivity.

$\sigma = AT^{3/2}\, exp(-E_g/KT)$ .....(10)

where σ is the electrical conductivity, A is constant, K is Boltzmann constant, and T is working temperature (T=310K). Using these three equations together, the final equation of sensing response can be derived and written as follows (see Table 4) [2].

$S = exp\,(|\Delta E_g|/KT) - 1$ .....(11)

Where S is sensing response and

$\Delta E_g = E_{g1} - E_{g2}$ and E_{g1} & E_{g2} are the energy gaps of the system and the complex, respectively.

3.4 Recovery time (τ)

A system's recovery time (τ) refers to the duration required for gas molecules to desorb from the surface. It offers valuable insights into the practical feasibility of systems, particularly in developing effective sensors. For optimal sensor performance, the τ should be neither too large nor too small, but at an optimal level. A more negative E_{ad} results in a larger τ, while a smaller E_{ad} is not conducive for

sensor materials. Therefore, achieving an optimal E_{ad} is crucial for attaining a feasible τ. The recovery time can be predicted with the following equation

$$\tau = \upsilon_0^{-1} exp\left(-\frac{E_{ads}}{kT}\right) \qquad \ldots\ldots\ldots(12)$$

Where T, K and υ_0 are the temperature (310K), the Boltzmann's constant (8.617×10^{-5} eVK^{-1}) and the attempted frequency (10^{15}) respectively.

Complex	τ (Sec)	S
CO/Cu_3Ni	2.20×10^{-6}	6.851
NO/Cu_6	2.71×10^{-12}	19.606
NH_3/Cu_4	1.22×10^{3}	18.950
NH_3/Cu_3Ag	3.85×10^{3}	21.421
NH_3/Cu_3Ni	1.55×10^{2}	14.383
NH_3/Cu_5Ni	8.45×10^{-1}	4.369

Table 4: Calculated Recovery Time (τ), and Sensing Response (S) for CO, NO and NH_3 gases and Cu_4, Cu_3Ag, Cu_3Ni, Cu_6, Cu_5Ag, and Cu_5Ni nanoclusters.

Table 4 presents the τ values for CO, NO, and NH_3 adsorbed Cu clusters. The CO-adsorbed Cu_3Ni cluster exhibits a τ value of 2.20 seconds, indicating its suitability for CO gas sensing. On the other hand, the NO-adsorbed Cu_6 and NH_3-adsorbed Cu_5Ni clusters demonstrate τ values of 2.71 seconds and 8.45 seconds, respectively, suggesting that Cu_6 is well-suited for NO gas molecule sensing. The NH_3 adsorbed Cu_4, Cu_3Ag, and Cu_3Ni clusters exhibit τ values of 1.22 seconds, 3.85 seconds, and 1.55 seconds, respectively. These relatively larger τ values imply the potential use of pristine Cu_4, Cu_3Ag, and Cu_3Ni clusters for removing NH_3 from the surroundings.

3.5 Global indices

In this section, we will concentrate on the characterization and analysis of various clusters using Density Functional Theory (DFT) reactivity descriptors. Reactivity is a fundamental electronic characteristic of a system, indicating its predisposition toward undergoing chemical change. Global reactivity descriptors serve as robust indicators for assessing this behavior. To have more idea about the system and biomolecule there are parameters namely global indices more specifically hardness, softness, chemical potential, and electrophilicity [58][59] are evaluated. The chemical potential (μ) represents the electron's tendency to escape from a system in thermodynamic equilibrium; a more negative μ implies a greater reluctance to lose an electron and an increased affinity for electron acquisition. The chemical hardness (η), on the other hand, quantifies the system's resistance to charge transfer, providing a measure of its inherent stability. The electrophilicity index (ω) quantifies the stabilization energy gained by the system when it becomes saturated with electrons from an external source. Together, these indices offer a comprehensive framework for evaluating a system's reactivity and stability.

The global indices can be defined as

$$\eta = \frac{I-A}{2} \quad \text{.....(13)}$$

$$\mu = -\frac{I+A}{2} \quad \text{.....(14)}$$

$$S = \frac{1}{2\eta} \quad \text{.....(15)}$$

$$w = \frac{\mu^2}{2\eta} \quad \text{.....(16)}$$

Where η, S, μ and W are hardness, softness, chemical potential and electrophilicity respectively. The parameters $I = -E_{HOMO}$ and $A = -E_{LUMO}$ as shown in Table 5.

Complex	μ (eV)	η (eV)	S $(eV)^{-1}$	W (eV)
CO/Cu_3Ni	-3.71 α	1.27 α	0.394 α	5.418 α
	-3.68 β	1.24 β	0.403 β	5.460 β
NO/Cu_6	-4.74 α	0.95 α	0.523 α	11.738 α
	-4.29 β	1.35 β	0.370 β	6.816 β
NH_3/Cu_4	-2.96	1.21	0.411	3.617
NH_3/Cu_3Ag	-3.01	1.25	0.400	3.624
NH_3/Cu_3Ni	-2.97 α	1.23 α	0.405 α	3.583 α
	-2.94 β	1.20 β	0.415 β	3.574 β
NH_3/Cu_5Ni	-3.49 α	1.54 α	0.325 α	3.954 α
	-3.37 β	1.42 β	0.352 β	3.998 β

Table 5: Global indices parameters Chemical potential (μ), Hardness (Ƞ), Softness(S) and Electrophilicity (W).

The change in the reactivity between the toxic gases and the pristine as well the doped clusters are very well understood by the global indices parameters. The chemical potential relates the energy changes when a system undergoes a chemical or physical reactions. It measures the potential tendency to react with the surroundings. The value of chemical potential changes maximum in the case of Cu_3Ni for the adsorption of NH_3 which changes from -3.801 to -2.94 eV for system and complex respectively which suits the adsorption energy value range. The parameter hardness will reflect the chemical stability of the system. This increases after the adsorption of gas molecules and also due to increment in the energy gap .

The range of Hardness of complex after interaction with gas changes notably in which hardness of CO/Cu_3Ni, NH_3/Cu_4, NH_3/Cu_3Ag, NH_3/Cu_3Ni complexes increases from 0.995, 0.949, 0.956, 0.995 eV to 1.270, 1.215, 1.250, 1.235 eV

respectively while the for NO/Cu_6, NH_3/Cu_5Ni decreases from 1.609, 1.630 eV to 1.540, 0.955 eV from their respective Nanoclusters before adsorption of gas molecule. As softness is inverse of hardness, it decreases due to the increment in hardness value. The complexes of NO/Cu_6, NH_3/Cu_5Ni becomes softer from their respective nanoclusters while CO/Cu_3Ni, NH_3/Cu_4, NH_3/Cu_3Ag, NH_3/Cu_3Ni becomes harder compared to its pristine. Next parameter electrophilicity which show the transfer of electron from atoms also get change significantly which is in accordance with the change in HOMO LUMO gap taking place after the adsorption of gas molecule over the nanoclusters. All values are presented in table 5.

CHAPTER IV
CONCLUSION

Conclusion

We present here DFT study of CO, NO, and NH_3 gas adsorption over Ni and Ag doped Cu_4 and Cu_6 nanoclusters. We have studied structural, electronic, vibrational properties of System as well as Complex after the adsorption of gas molecules. As a result of the negative formation and binding energies and the absence of the imaginary frequency (IR plot), the pristine Cu_4 and Cu_6 nanoclusters are structurally and dynamically stable. Adsorption of CO, NO and NH_3 gas molecules shows that CO/Cu_3Ni, NO/Cu_6, NH_3/Cu_4, NH_3/Cu_3Ag, NH_3/Cu_3Ni, and NH_3/Cu_5Ni do not exhibit imaginary modes, indicating that they are dynamically stable. CO-adsorbed Cu_3Ni cluster indicates high potential for CO gas sensing applications. Pristine Cu_4, Cu_3Ag, and Cu_3Ni clusters can be used for removing NH_3 from the surroundings.

CHAPTER V

REFERENCES

References

[1] Xin Ge , Shuhuan Zeng , Hongwen Deng , Boon K. Teo , Cunfa Sun , Atom-precise copper nanoclusters based on FCC, BCC, and HCP structures, Coordination Chemistry ,503 (2024) 215667, https://doi.org/10.1016/j.ccr.2024.215667.

[2]Ashvin Kanzariya , Shardul Vadalkar , Sourav Kanti Jana , L.K. Saini , Prafulla K. Jha , An *ab-initio* investigation of transition metal-doped graphene quantum dots for the adsorption of hazardous CO2, H2S, HCN, and CNCl molecules, Journal of Physics and Chemistry of Solids ,186 (2024) 111799, https://doi.org/10.1016/j.jpcs.2023.111799.

[3] Mitchell, S., Qin, R., Zheng, N. *et al.* Nanoscale engineering of catalytic materials for sustainabletechnologies,*Nat.Nanotechnol*,129–139(2021)16, https://doi.org/10.1038/s41565-020-00799-8.

[4] Jay Panchal , Apeksha Gauswami , Darshil Chodvadiya , Harendrasinh Jadeja , Prafulla K. Jha ,Adsorption performance of CO, NO and NH3 hazardous gas molecules over B9N9 and Al9N9 nanorings: Acumen from density functional theory , Materials Chemistry and Physics, 311 (2024) 128565, https://doi.org/10.1016/j.matchemphys.2023.128565.

[5] C.P. Wang, Z. Wang, S.J. Mao, Z.R. Chen, Y. Wang, Coordination environment of active sites and their effect on catalytic performance of heterogeneous catalysts Chinese J. Catal, 43 (2022) 928–955, 10.1016/S1872-2067(21)63924-4

[6] Z. Li, S. Ji, Y. Liu, X. Cao, S. Tian, Y. Chen, Z. Niu, Y. Li, Well-Defined Materials for Heterogeneous Catalysis: From Nanoparticles to Isolated Single-Atom Sites Chem. Rev, 120 (2020) 623–682 https://doi.org/10.1021/acs.chemrev.9b00311

[7] Wang, J.; Lin, X.; Shu, T.; Su, L.; Liang, F.; Zhang, X. Self-Assembly of Metal Nanoclusters for Aggregation-Induced Emission, *Int. J. Mol. Sci.* **2019**, *20*(8), 1891; **https://doi.org/10.3390/ijms20081891**

[8] X. Liu, D. Astruc, Atomically precise copper nanoclusters and their applications*Coord. Chem. Rev,(* 2018), **359**, 112. https://doi.org/10.1016/j.ccr.2018.01.001

[9] Lin Y. S.; Lin Y. F.; Nain A.; Huang Y. F.; Chang H. T, A critical review of copper nanoclusters for monitoring of water quality, Sens. Actuators Rep. 2021 3, 100026, 10.1016/j.snr.2021.100026.

[10] Jebran Ahmad , Muhammad Yaseen , Tanveer ul Haq Zia , Muhammad Ali , Latif Ur Rahman , Ata Ur Rahman, Designing copper–nickel hybrid nanoparticles based resistive sensor for ammonia gas sensing, Materials Chemistry and Physics ,305 (2023) 127868, https://doi.org/10.1016/j.matchemphys.

[11] Yong-jin Peng , He Huang , Chang-jun Wang , DFT investigation on electronic structure, chemical bonds and optical properties of Cu6(SR)6 nanocluster , Chemical Physics Letters 780, (2021) 138898, https://doi.org/10.1016/j.cplett.2021.138898.

[12] A. Baghdasaryan, R. Grillo, S.R. Bhattacharya, M. Sharma, E. Reginato, H. Theraulaz, I. Dolamic, M. Dadras, S. Rudaz, E. Varesio, T. Burgi, ACS Appl. Nano Mater. 2018, 1, 8, 4258–4267 https://doi.org/10.1021/acsanm.8b01049

[13] K. Basu, S. Paul, R. Jana, A. Datta, A. Banerjee, ACS Sustainable Chem. Eng. 2019, 7, 2, 1998–2007 https://doi.org/10.1021/acssuschemeng.8b04301

[14] J. Zheng, J. Wang, D. Song, J. Xu, M. Zhang, ACS Appl. Nano Mater. 2020, 3, 4, 3449–3458 https://doi.org/10.1021/acsanm.0c00194

[15] D. Li, G. Wang, L. Cheng, C. Wang, X. Mei, ACS Omega 2018, 3, 11, 14755–14765 https://doi.org/10.1021/acsomega.8b02204

[16] Y. Liu, Q. Li, R. Si, G.-D. Li, W. Li, D.-P. Liu, D. Wang, L. Sun, Y. Zhang, X. Zou, oupling Sub-Nanometric Copper Clusters with Quasi-Amorphous Cobalt Sulfide Yields Efficient and Robust Electrocatalysts for Water Splitting Reaction Adv. Mater,29 (2017) 1606200. 10.1002/adma.201606200

[17] S. Zhou, F. Wang, C. Wang, Recent progress in the synthesis of luminescent copper clusters Advances In Nano Research 4 ,(2016) 113. 10.12989/anr.2016.4.2.113.

[18] M. Wang, S. Wang, D. Su, X. Su, Copper nanoclusters/polydopamine nanospheres based fluorescence aptasensor for protein kinase activity determination Anal. Chim. Acta 1035 ,(2018) 184. 10.1016/j.aca.2018.06.043

[19] Z. Liu, X. Jing, S. Zhang, Y. Tian, A Copper Nanocluster-Based Fluorescent Probe for Real-Time Imaging and Ratiometric Biosensing of Calcium Ions in Neurons.Anal. Chem. 91 ,(2019) 2488. 10.1021/acs.analchem.8b05360

[20] K. Nakamae, T. Nakajima, Y. Ura, Y. Kitagawa, T. Tanase, Facially DispersedPolyhydride Cu 9 and Cu 16 Clusters Comprising Apex-Truncated Supertetrahedral and Square-Face-Capped Cuboctahedral Copper Frameworks Angewandte Chemie- International Edition 59 ,(2020) 2262, https://doi.org/10.1002/anie.201913533.

[21] Z. Wang, Y. Xiong, S.V. Kershaw, B. Chen, X. Yang, N. Goswami, W.-F. Lai, J. Xie,A.L. Rogach, In Situ Fabrication of Flexible, Thermally Stable, Large-Area, Strongly Luminescent Copper Nanocluster/Polymer Composite Films, Chem. Mater. 29, (2017) 10206, https://doi.org/10.1021/acs.chemmater.7b04239.

[22] K. Basu, K. Gayen, T. Mitra, A. Baral, S.S. Roy, A. Banerjee, Different Color Emissive Copper Nanoclusters for Cancer Cell Imaging, ChemNanoMat 3, (2017) 808, https://doi.org/10.1002/cnma.201700162.

[23] X. Liu, D. Astruc, Atomically precise copper nanoclusters and their applications, Coord. Chem. Rev. 359, (2018) 112, https://doi.org/10.1016/j.ccr.2018.01.001.

[24] A. Shah, R. Qureshi, S.B. Khan, A.M. Asiri, A.-u.-H.A. Shah, M. Ishaq, M.S. Khan, S. K. Lunsford, M.A. Zia, Engineering, Spectroscopic analysis of Au-Cu alloy nanoparticles of various compositions synthesized by a chemical reduction method, Adv. Mater. Sci. Eng,(2015), https://doi.org/10.1155/2015/638629 .

[25] L.-u. Rahman, R. Qureshi, M.M. Yasinzai, A. Shah, Synthesis and spectroscopic characterization of Ag-Cu alloy nanoparticles prepared in various ratios, C. R. Chim. 15 (2012) 533–538 https://doi.org/10.1016/j.crci.2012.03.012.

[26] W. Weihua, T. Xuelin, C. Kai, C. Gengyu, Synthesis and characterization of Pt–Cu bimetallic alloy nanoparticles by reverse micelles method, Colloid. Surface, 273 (2006) 35–42, https://doi.org/10.1016/j.colsurfa.2005.07.029.

[27] N. Krishnankutty, N.M. Rodriguez, R.T.K. Baker, J. Catal, Effect of copper on the decomposition of ethylene over an iron catalyst , 158 (1996), 217-227, https://doi.org/10.1006/jcat.1996.0021.

[28] Y.T. Shah, A.J. Perrotta, Catalysts for Fischer-Tropsch and iso synthesis Prod. R&D, 15 (1976), 123-131, https://doi.org/10.1021/i360058a005.

[29] T. Inoue K. Yamauchi, F. Fujita Effects of alloying element balance and micro-alloying elements on magnetic properties and hot ductility of PC permalloy Mater.
Trans, 49 (2008), 650-654 10.2320/matertrans.MER2007235

[30] S. Datta, T. Saha-Dasgupta, Structural, electronic and magnetic properties of transition metal binary alloy clusters with isoelectronic components: case study with MnmTcn, TimZrn and MnmRen J. Phys. Condens. Matter: Inst. Phys. J, 25 (2013), 225302. 10.1088/0953-8984/25/22/225302

[31] L. Rout, A. Kumar, R.S. Dhaka, P. Dash ,Bimetallic Ag-Cu alloy nanoparticles as a highly active catalyst for the enamination of 1,3-dicarbonyl compounds RSC Adv, 6 (2016), 49923-49940. 10.1039/C6RA04569C

[32] J. Xu, D. Bhattacharyya ,Membrane-based bimetallic nanoparticles for environmental remediation: synthesis and reactive properties Environ. Prog, 24 (2005), 358-36. 10.1002/ep.10106

[33] Xu, Haiping; Rebollar, Dominic; He, Haiying; Chong, Lina; Liu, Yuzi; Liu, Cong; Sun, Cheng-Jun; Li, Tao; Muntean, John V.; Winans, Randall E.; Liu, Di-Jia; Xu, Tao, Highly selective electrocatalytic CO2 reduction to ethanol by metallic clusters dynamically formed from atomically dispersed copper Nature Energy (2020), 5 (8), 623-632CODEN: NEANFD; 2058-7546. 10.1038/s41560-020-0666-x

[34] Yun, W. S. & Lee, J. D. Unexpected strong magnetism of Cu doped single-layer MoS2and its origin. *Phys. Chem. Chem. Phys.***16,** 8990–8996 (2014). 10.1039/c4cp00247d

[35] T. Holtzl, N. veldeman, T. Veszpremi, P. Lievens, M.T. Nguyen, Cu6Sc+ and, Cu_5Sc : Stable, high symmetry and aromatic scandium-doped coinage metal clusters Chem. Phys. Lett.,469 (2009), 304-307. https://doi.org/10.1016/j.cplett.2009.01.001

[36] V.E. Matulis, D.M. Palagin, A.S. Mazheika, O.A. Ivashkevich, DFT study of electronic structure and geometry of anionic copper clusters Cu^-_n (n = 11, 12, 13) J. Mol. Struct. (Theochem), 857 (2008), 66-71. 10.1016/j.theochem.2008.02.005

[37] Sadegh Kaviani , Irina I. Piyanzina , Oleg V. Nedopekin , Dmitrii A. Tayurskii, Adsorption behavior and sensing properties of toxic gas molecules onto PtnBe (n = 5, 7, 10) clusters: A DFT benchmark study, Materials Today Communications, 33 (2022) 104851, https://doi.org/10.1016/j.mtcomm.2022.104851.

[38] S. Rattan, S. Kumar, J.K. Goswamy, Gold nanoparticle decorated graphene for efficient sensing of NO2 gas, Sens. Int, 3 (2022), 100147. https://doi.org/10.1016/j.sintl.2021.100147

[39] A. Palliyarayil, P.S. Prakash, S. Nandakumar, N.S. Kumar, S. Sil, Palladium nanoparticles impregnated activated carbon material for catalytic oxidation of carbon monoxide, Diam. Relat. Mater, 107 (2020), 107884. https://doi.org/10.1016/j.diamond.2020.107884

[40] R. Leghrib, T. Dufour, F. Demoisson, N. Claessens, F. Reniers, Gas sensing properties of multiwall carbon nanotubes decorated with rhodium nanoparticles, Sens. Actuators B Chem, 160 (2011) 974–980. https://doi.org/10.1016/j.snb.2011.09.014

[41] Megha ,A. Banerjee, T.K. Ghanty, Adsorption and activation of CO2 molecule on subnanometer-sized anionic vanadium carbide clusters VnC4 (n = 1–6): a theoretical study, Mol. Catal, 515 (2021), 111871. https://doi.org/10.1016/j.mcat.2021.111871

[42] S.D. Baruah, N.K. Gour, P.J. Sarma, R.C. Deka, DFT insight on oxygen adsorbed platinum trimer cluster (Pt3) for CO oxidation, Comput. Theor. Chem,1114 (2017) 1–7.

https://doi.org/10.1016/j.comptc.2017.05.023

[43] Mei-Yin Yen, Jia-Jen Ho Density-functional study for the NOx (x = 1, 2) dissociation mechanism on the Cu(1 1 1) surface, Chemical Physics, 373 (2010) 300–306, doi:10.1016/j.chemphys.2010.06.005.

[44] F. Illas, J.M. Ricart, M. Fernández-García, Geometry, vibrational frequencies and bonding mechanism of NO adsorbed on Cu(111) J. Chem. Phys, 104 (1996) 5647. https://doi.org/10.1063/1.471773

[45] A.R. Balkenende, O.L.J. Gijzeman, J.W. Geus, The interaction of NO and CO with Cu(111)Appl. Surf. Sci, 37 (1989) 189. https://doi.org/10.1016/0169-4332(89)90482-0

[46] P. Dumas, M. Suhren, Y.J. Chabal, C.J. Hirschmugl, G.P. Williams, Adsorption and reactivity of NO on Cu(111): a synchrotron infrared reflection absorption spectroscopic study Surf. Sci, 371 (1997) 200. https://doi.org/10.1016/S0039-6028(96)00987-9

[47] S. González, C. Sousa, F. Illas, Adsorption and reactivity of NO on Cu(111): a synchrotron infrared reflection absorption spectroscopic studyJ. Catal, 239 (2006) 431. https://doi.org/10.1016/j.jcat.2006.02.013

[48] M.J. Frisch, G.W. Trucks, H.B. Schlegel, G.E. Scuseria, M.A. Robb, J.R. Cheeseman, G. Scalmani, V. Barone, B. Mennucci, G.A. Petersson, et al., Gaussian 09, RevisionD.01, Gaussian Inc., Wallingford, CT, 2013.

[49] S. Grimme, J. Antony, S. Ehrlich, H. Krieg, A consistent and accurate ab initio parametrization of density functional dispersion correction (DFT-D) for the 94 elements H-Pu, J. Chem. Phys. 132 (2010), doi:10.1063/1.3382344.

[50] M. Kurban, İ. Muz, Theoretical investigation of the adsorption behaviors of fluorouracil as an anticancer drug on pristine and B-, Al-, Ga-doped C36 nanotube, J. Mol. Liq, 309 (2020), https://doi.org/10.1016/j.molliq.2020.113209.

[51] Sainda, Riddhi, et al. The First-Principles investigation of sensing and removal applications of nitrobenzene using pristine and Sc decorated B9N9 nanoring, Journal of Molecular Liquids, 409 (2024), 125389. https://doi.org/10.1016/j.molliq.2024.125389

[52] C. Parlak, Ö. Alver, Single and double silicon decoration of fullerene C60 and single walled carbon nanotubes for adsorption and detection of TNT, J. Mol. Struct, 1198 (2019), https://doi.org/10.1016/j.molstruc.2019.126881.

[53] M. Shahabi, H. Raissi, F. Mollania, Electronic structures, intramolecular hydrogen bond interaction, and aromaticity of substituted 4-amino-3-penten-2-one in ground and electronic excited state, Struct. Chem, 26 (2015) 491–506,https://doi.org/10.1007/s11224-014-0505-4.

[54] M. Shahabi, H. Raissi, Investigation of the molecular structure, electronic properties, AIM, NBO, NMR and NQR parameters for the interaction of Sc, Ga and Mg-doped (6,0) aluminum nitride nanotubes with COCl2 gas by DFT study, J. Incl. Phenom. Macrocycl. Chem, 84 (2015) 99–114,https://doi.org/10.1007/s10847-015-0587-7.

[55] Tukadiya, Namrata A., et al,C24 Fullerene and its derivatives as a viable glucose sensor: DFT and TD-DFT studies, Surfaces and Interfaces 41 (2023), 103220. https://doi.org/10.1016/j.surfin.2023.103220

[56] Jiang, Jinhua, et al, A DFT study on the effect of Au-decoration on the interaction of adrucil drug with BC2N nanotubes in the gas phase and aqueous solution, *Journal of Molecular Liquids* 315 (2020), 113741. https://doi.org/10.1016/j.molliq.2020.113741

[57] Yang, Yuping, Aili Sun, and Majid Eslami,A density functional theory study on detection of amphetamine drug by silicon carbide nanotubes, *Physica E: Low-dimensional Systems and Nanostructures* ,125 (2021), 114411. 10.1016/j.physe.2020.114411

[58] Jana, Sourav Kanti, et al, A quantum mechanical prediction of C24 fullerene as a DNA nucleobase biosensor, *Diamond and Related Materials* ,129 (2022): 109305. 10.1016/j.diamond.2022.109305

[59] S. Vadalkar, D. Chodvadiya, N.N. Som, K.N. Vyas, P.K. Jha, B. Chakraborty, An Ab-initio Study of the C18 nanocluster for Hazardous Gas Sensor Application, ChemistrySelect. 7 (2022), https://doi.org/10.1002/slct.202103874.